UNIVERSITA' DELLA CALABRIA

Dipartimento di Fisica

Scuola di dottorato "Bernardino Telesio" - Scuola di Scienza e Tecnica

Fisica dei sistemi complessi

XXV CICLO

A Lévy Walk approach to the propagation of solar energetic particles

Settore Scientifico Disciplinare FIS/05

Direttore: Ch.mo Prof. Roberto Bartolino

Firma _____

Supervisore: Ch.mo Prof. Gaetano Zimbardo

Firma _____

Dottorando: Dott. Enrico Maria Trotta

Firma _____

A volte è tropppo tardi…
ciao Papà

Massiccio del Pollino

"Io dico l'universo tutto infinito, perché non ha margine, termine, né superficie; dico l'universo non essere totalmente infinito, perché ciascuna parte che di quello possiamo prendere, è finita, e de mondi innumerabili che contiene, ciascuno è finito. Io dico Dio tutto infinito, perché da sé esclude ogni termine ed ogni suo attributo è uno ed infinito…

… Uno dunque è il cielo, il spacio immenso, il seno, il continente universale, l'eterea regione per la quale il tutto discorre e si muove. Ivi innumerabili stelle, astri, globi, soli e terre sensibilmente si veggono, ed infiniti raggionevolmente si argumentano. L'universo immenso ed infinito è il composto che resulta da tal spacio e tanti compresi corpi."

[G. Bruno], "De l'Infinito Universo e mondi" - Dialogo I, III (1584)

Massiccio del Pollino

ABSTRACT

A Lévy Walk approach to the propagation of solar energetic particles

Dr. Enrico Maria Trotta
Department of Physics - Doctorate School B.Telesio
Physics of Complex Systems (FIS/05 - Astronomy and Astrophysics)

This thesis is dedicated to the problem of energetic particle propagation in the solar wind, with special emphasis on the propagation of solar energetic particles (SEPs). Those particles are accelerated either in the low corona by flares, usually giving rise to so-called impulsive SEP events, or in the higher corona by the shock driven by coronal mass ejections, giving rise to the so-called gradual SEP events. In either case, energetic particles propagate in the solar wind along the spiral magnetic field, and then reach the Earth's environment, where they can intensify the auroral emission and downgrade or even damage spacecraft operations. Indeed, SEPs represent one of the major hazards of the research programme known as space weather, which aims at reducing the risks associated with the solar and space activities.

The fluxes of energetic particles measured in the Earth's environment depend both on the source strength and on the propagation properties. Traditionally, two limiting transport regimes are considered, that is, diffusive transport and scatter-free, i.e., ballistic, transport. However, in the last two decades, anomalous transport regimes in which the mean square displacement grows nonlinearly with time have become more and more common. An anomalous transport regime, either subdiffusive or superdiffusive, would influence in a fundamental way the flux of solar energetic particles reaching the Earth. To study this problem we have developed two approaches, one based on the analysis of SEP fluxes measured by spacecraft in the solar wind, and the other on the numerical simulation of SEPs in the case of superdiffusive transport.

In the first approach, we considered SEPs measurements by ACE, Wind and other spacecraft for the case ofi mpulsive SEP events, and compared the time profile of the energetic particles with that corresponding to the different forms which the propagator assumes in the case of superdiffusive transport. The comparison gives direct information on the transport regime, showing that electrons propagate in a superdiffusive way with anomalous diffusion exponent alpha running from 1.2 to 1.75. For protons, quasi-ballistic transport regimes are also found.

In the second approach, the statistical mechanism giving rise to superdiffusion, namely the Lévy random walk, is investigated numerically. We developed a new numerical code which simulates the Lévy walk while changing the parameters which determine the pace of transport, that is the exponent of the power law tails of the jump probability distribution. This code reproduces well the anomalous transport predictions for the mean square displacement and for the propagator of Lévy walks, while allowing a clear and simple identification of the parameters determining the transport regime. Therefore this code represents a powerful tool to compare the simulation results to spacecraft data.

Comparison with the data has been considered both for impulsive and gradual SEP events. In this thesis, we show that the numerical code reproduces well the observations ofi mpulsive events for the various transport regimes. Additional work is required to apply the code to the propagation of gradual SEP events, as modeling of the shock source is required. While this will be implemented in the near future, the effectivitiy of the numerical code will allow an important improvement in the understanding of SEP propagation and in the prediction of space weather perturbations.

Keywords: Solar Energetic Particles propagation, Transport theory in solar wind, Lévy walks, Anomalous Diffusion

Contents

Chapter 1

Introduction

The Sun is an active star and is a powerful source of energetic particles, which are accelerated in short time, to energies from a few MeV to a few GeV. These particles propagate from the Sun to the Earth moving along the solar wind magnetic field. The study of the propagation of energetic particles from the sun is of particular importance in the discipline of space weather, which aims to prevent/predict the effects of solar activity and disturbances in the interplanetary space on the terrestrial environment and on those high technology structures that may be affected by the phenomena described below. The theoretical framework used to describe the motion of particles is the theory of diffusive transport, which builds on the formalization of random events by using the laws of probability.

In 1905, the journal Nature published a famous exchange of letters between Karl Pearson and Lord Rayleigh on the possibility to study the rate of spread of malaria. In particular, Pearson was studying the phenomenon hoping to solve this problem by integrating the probability of being at a certain distance from a starting point taking steps of equal length in random directions. Having failed to obtain an explicit expression beyond the second step, he decided to ask for help from the readers of the magazine coining, for the occasion, the famous example of a drunk man who moves unsteadily, and with it the expression of random walk. Among the many responses he received,

there was that of Lord Rayleigh, who claimed to have already studied and solved the equivalent problem of the propagation of a sound wave in a homogeneous medium, obtaining the explicit solution in the limit of infinite steps. This led to reconsider the approach attempted so far in the study of random walks. A similar operation of limit is applicable to the way in which light propagates: on its way from the Sun through the Earth's atmosphere it encounters a huge number of atoms, molecules and particles distributed in a homogeneous and disorderly manner and that complicate the propagation, otherwise straight, with phenomena of reflection, refraction, diffraction, absorption and re-emission. In this way, the perceived light can usually also have very different characteristics from those of departure and, with their study, it is possible to infer a lot of physical information on the emitting and propagation media.

The random walks that are obtained in this way have been studied for over a century in areas that go far beyond the simple propagation of light, as with this model it is possible to take into account, using suitable assumptions, many properties of complex systems. These assumptions concern substantially the probability that the increments have certain characteristics, expressed by their distribution function. For a long time, the necessary assumptions to be made on the distribution of "steps" of the random walk have remained the same, as they were general enough to be able to describe and find application in a wide range of situations. If, for instance, as in the case of Pearson's drunk man, the increments are independent and all more or less of the same entity, the resultant random walk still has apparently surprising characteristics: because there are no preferential directions for the various shifts, the position reached after a number of steps will tend to coincide with that of departure. Nevertheless, with the passage of time, following this type of path it will be possible to explore all the surrounding space passing infinite number of times for each point on the surface where the motion occurs. The trajectory described above is generally referred to with the name of Brownian motion, and, the slow growth of the distance explored on average by the walker that runs it, arises from general assumptions that take the name of normal diffusion.

Starting from the concept of random walk as the sum of identically distributed independent variables, it is feasible to describe the phenomena of normal diffusion. Referring to the generalization of the Lévy and Gnedenko of the Theorem of the central limit, the normal diffusion becomes a limiting case of the broader class of phenomena of anomalous diffusion. This category includes the possibility of spreading in a much faster way, and is linked to a type of trajectories called Lévy flights and Lévy walks which, also having very different characteristics from those of the Brownian motion, are finding application in the description of an increasing number of systems.

The aim of this thesis is to analyze both the mode of propagation of energetic particles generated by impulsive events in the solar corona, and the definition of a numerical model for the study of Lévy distribution properties (Lévy Random Walk). In particular, in the first part of the paper we analyze *purely* impulsive events, or rather referable to individual physical phenomena (flare), in order to show the characteristics of the transport regimes of impulsive isolated events. In the second part, we have developed an algorithm for the simulation of the distributions of Levy. The analysis of the diffusive regimes for impulsive events was carried out by developing a methodology, based on the analysis and integration of various experimental data (data from several satellites) and on the verification of theoretical models describing the different transport regimes through the use of propagators.

1.1   Space Weather

The energetic particles play an important role in relation to the effects of their interaction with equipment in orbit and the Earth's magnetosphere. Because of these effects, it has been formed a research field called *Space Weather*, whose objective is *the study of the conditions of the Sun,*

the solar wind, the magnetosphere, ionosphere and thermosphere for forecasting their effects on human activities (U.S. National Space Weather program). The geomagnetic storms, the destruction of satellites due to their interaction with very energetic particles, and also the very frequent problems in the communication system during the maximum of the solar cycle, are largely caused by Coronal Mass Ejection (CMEs). This is why the interest in CMEs, flares and phenomena associated with the release of energetic particles, goes beyond the astrophysics field, and also aims at the possibility to predict their occurrence to, eventually, limit any effects on Earth.

In other words, the mass expulsion of the corona along with the flares can disrupt radio transmissions, creating power cuts (blackouts), damage to satellites and electric transmission lines. To summarize the objectives and terms of reference for the space weather, it can be described in relation to the following categories:

- Main physical parameters involved

    – Number of sunspots

    – Solar flow in radio band

    – Geo-magnetism

- Phenomena under study

    – Sun (emission of radiation and coronal mass)

    – Terrestrial Magnetism

    – Ionosphere, Thermosphere

    – Interplanetary space

    – Solar Cycle

- Impacts on human activities

  – Telecommunications

  – Electricity Distribution

  – Commercial flights of long duration

  – Mining and oil exploration

  – Tourism

  – Health

1.2 Propagation of energetic particles

There are many phenomena that generate fluxes of energetic particles in the interplanetary space: the flares in the low solar corona, Coronal Mass Ejection (CME) and the shock waves in Corotating Interaction Regions (CIR). The flare is a loud explosion that involves a huge amount of energy. The phenomenon was observed for the first time in on the sun, by the British astronomer Richard Carrington, in 1859. In more recent times, the flares have been observed on many other stars. These phenomena, which represent the most "eye-catching" between the solar activity (Figure 1), are eruptive events that start in the area between the lower corona and the photosphere, then extending towards the corona. The explosions occur mainly above sunspot groups, areas of high magnetic activity, and are probably caused by the release of energy on the occasion of the phenomenon of reconnection of magnetic field lines. The flare is manifested at the level of the chromosphere through the loops, tubes of magnetic flux shaped as an arc representing the typical structure of the solar magnetic field of the active zones of the sun. Mass expulsions, called Coronal Mass Ejection (CME), are produced instead at the level of the corona, that may reach the interplanetary scale, the Earth's magnetosphere and extend up to the regions furthest from the Sun, giving rise, among

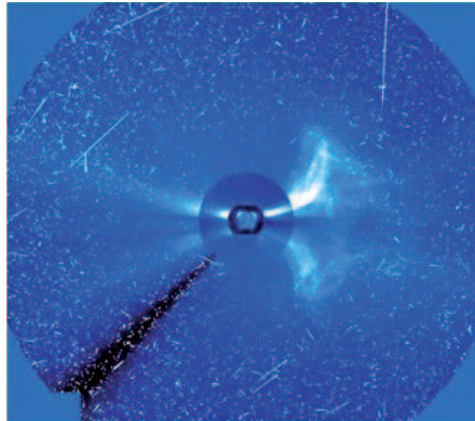other things, to northern and southern Lights.

Figure 1.1 Solar Energetic Particles related to a CME
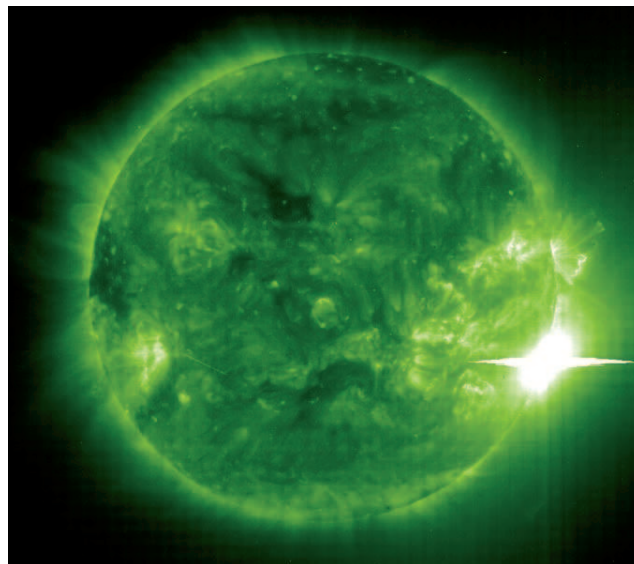
1.2.1 Flares

Figure 1.2 UV image of a flare from SOHO

The flares have a variable frequency: from many per day, when the Sun is particularly *active*,

to about one per week, when it is *quiet*. The flare takes many hours or even days to *charge*, but the blast itself takes a few minutes to release its energy. The resulting shock waves travel laterally through the photosphere and upward through the chromosphere and the corona, at speeds of $1000 - 2000 Km/s$. The flares are classified according to their power in $A, B, C, M or X$, normally solar activity is between classes $A and C$. In particular, the classification is built in relation to the intensity of the emission at the wavelength of X-rays emitted (from 1 to 8 Angtrom) and measured in Earth orbit. Each class $A, B, C, M and X$ is divided into nine sub-categories (i.e. from A1 to A9, M1 to M9, etc..). Classes are on a logarithmic scale, hence a flare of class M is 10 times stronger than a flare of class C. The flare of class A - C produce little effects on the Earth, while

Class	Intensity (W/m^2)
A	$< 10^{-7}$
B	$>= 10^{-7} and < 10^{-6}$
C	$>= 10^{-6} and < 10^{-5}$
M	$>= 10^{-5} and < 10^{-4}$
X	$>= 10^{-4}$

Table 1.1 Summary Table for the power of the Flare.

the more powerful, M and X, have more serious consequences, even perceptible from our planet. The cycle of development of the flare can be summarized as follow: the plasma is heated up to temperatures of millions of degrees, while some particles reach relativistic energies, some of these particles collide with the heavy ions of the solar plasma and slow down, producing X-rays, which are then observed from the satellites. This phenomenon of braking radiation is known as the collisional bremsstrahlung of the electrons with the ions of the plasma, and results in an emission of electromagnetic energy. We may ultimately distinguish four subsequent phases in the development of a flare, in relation to the radiation emitted:

- the pre-flare phase of the duration of ten minutes, characterized by the emission of soft X-rays, or rays with energy less than 10keV. At this stage, it is also detectable a powerful heating of the plasma in the solar corona;

- the impulsive phase, which has a duration of about one minute. In this phase electrons and ions are strongly accelerated, it follows, therefore, an increase of emission of harsh X radiations and microwaves;

- the flash phase, of an average duration of five minutes, in which there is a rapid increase of the intensity of the radioactive emissions and of the solar area in which such emissions take place;

- the last stage, the longest, is the main phase characterized by a slow decrease in intensity which can last from an hour to a day, depending on the size of the event.

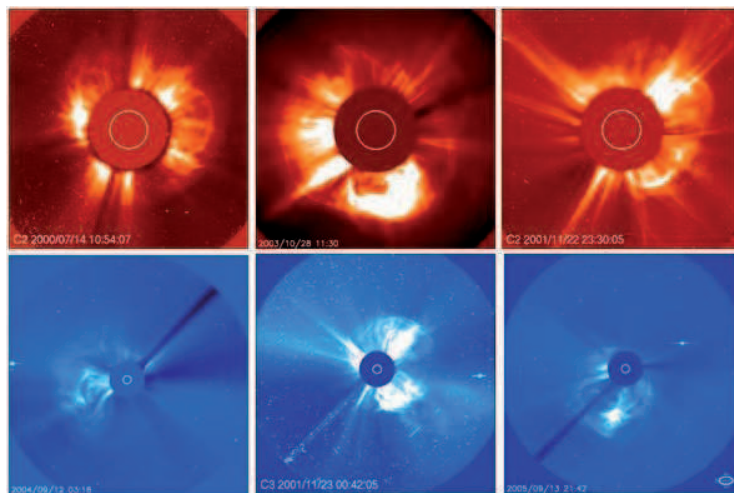### 1.2.2 Coronal Mass Ejection (CME)

Figure 1.3 CME *Halo Event* (Images from SOHO - LASCO c2 and c3)

Another phenomenon which gives rise to the emission of fluxes of energetic particles is the Coronal Mass Ejection (CME). CMEs are phenomena that originate from the explosion of magnetically confined structures, and their effect is to expel plasma, at speeds up to 1-2 thousand km / sec, in the solar atmosphere and into interplanetary space. It is thought that they have an important role in the reconfiguration of the solar magnetic field. Their frequency varies during the solar cycle from one event every two days at least, up to three events per day in the phase of maximum activity. The phenomenon has its origin in the solar corona and is observed by means of special instruments called coronagraphs. The ejected material, dragged by the magnetic field of the corona, mainly consists of electrons and protons in addition to small amounts of heavier elements such as helium, oxygen and iron.

The clouds of plasma ejected interact with the magnetosphere when they reach the earth, causing the phenomenon of the aurora borealis. Although the corona of the Sun was observed during total solar eclipses for thousands of years, the existence of CME has been discovered only recently. So that while the flare is a loud explosion that involves a huge amount of energy, Coronal Mass Ejection (CME) are produced instead at the level of the corona, that may reach the interplanetary scale, the Earth's magnetosphere and extend up to the regions furthest from the Sun, giving rise, among other things, to northern and southern Lights.

The phenomena described above are of particular relevance for the generation of SEP (Solar Energetic Particles). These particles, which may be accelerated to energies up to 1000 MeV, give information about the nature, composition and location of their source. High-energy particles from the Sun have been observed for the first time in February and March 1942 ie before the discovery of CME. For this reason, it was natural to assume that the sources of these particles were the only flare. The study of the SEP was then conditioned by this hypothesis, modeling the phenomenon in terms of particles injected at a certain moment in a point in space. The analysis of the phenomenon was conducted in terms of transport from a source point rather than as a feature of the acceleration

of the source at a certain instant. The change of perspective had with the discovery of the CME is well summarized in the figure below (Figure 1.4):
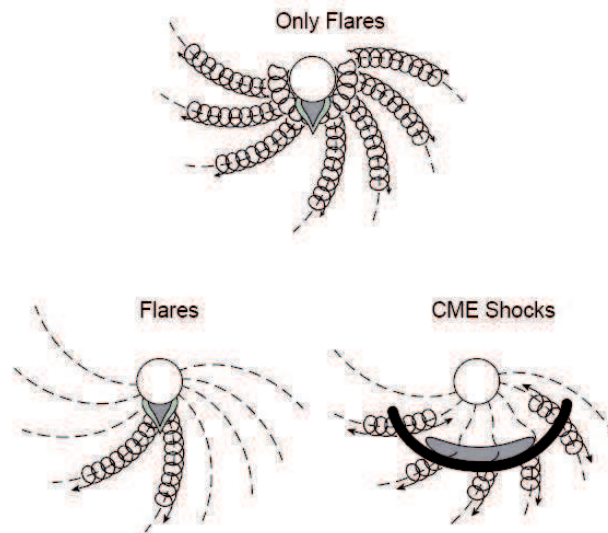

Figure 1.4 Change of perspective: from flare to flare + CME (Reames 1999)

The first evidence that two distinct acceleration processes contribute to the formation of SEP events came thanks to the observations of radio waves (Wild et al., 1963). The emission frequency in the radio explosions ("radio bursts") is related to the frequency of the local plasma, which varies as the square root of the electron density. For this reason, the fast frequencies shift of the radio burst of type III is linked to the electron beams from 10-100 keV from the corona, at speeds of about $0.1c$, generated by impulsive flare crossing plasma of decreasing density. On the other hand, radio burst of type II have the lowest rate of frequency shift, which correspond to acceleration of electrons to speeds of the order of 1000 km / s generated by shock waves that move through the corona. Wild hypothesized that electrons were accelerated in the impulsive phase of an event which produces radio burst type III, while the acceleration of protons occurs subsequently, i.e. during the expansion of the shock wave. In the years following the discovery of CMEs, SEP events were studied using X-ray data taking, in 1970, to a classification of events in impulsive and gradual

(Pallavicini et al, 1977): the first associated with the flare, the second with the CME. The evidence that allow to distinguish the two types are different: analysis of X-rays which show, for the two types of events, different ratios electrons/protons (Cane et al. (1986)) analysis of the abundances of isotopes ^3He and ^4He that show a peak in the abundance of ^3He for impulsive events (Hsieh and Simpson (1970)) advent of observation from artificial satellites. The first evidence of these events were obtained from observations made with a coronagraph from 1971 to 1973. A coronagraph produces an *artificial* eclipse of the Sun through a record of concealment superimposed on the image of the sun. Differently from natural events, the use of the coronagraph offers the possibility to observe the corona for long times, hence being able to appreciate the coronal changes at the base of the phenomenon of CME. Among the tools that contributed to the observation of CME, we can mention LASCO (Large Angle and Spectrometric Coronograph) installed on SOHO (Solar and Heliospheric Observatory). Using this tool it is possible to see "halo event", or else CME events directed towards the ground.

1.3   Aims of the works

The aim of this work is the analysis of the different transport regimes related to the propagation in the solar wind of solar energetic particles (SEPs) generated by impulsive events like solar flares and to compare the experimental energetic particle fluxes with the numerical simulation in order to investigate the different transport regime of energetic particles. A numerical implementation of a Lévy random walk for parallel particle transport is developed, which allows to obtain superdiffusive transports. These anomalous regime are important for the mechanism of energetic particle acceleration and for space weather predictions. A first set of numerical simulations show how nondiffusive motion can be generated by probability distribution of jump lengths in power law form. This probability distribution will be included into test particle simulation to study the propagation

of energetic particles in the heliosphere. The comparison between the flows measured by satellites and fluxes extracted from the numerical simulation, will contribute to a deeper understanding of the mechanisms underlying the presence of superdiffusive regimes of SEP transport in interplanetary medium. We carry out an analysis of the different transport regimes related to the propagation of solar energetic particles (SEPs) generated by impulsive events like solar flares (e.g., Reames (Reames 1999)). The analysis of experimental data (e.g., particle fluxes observed by SOHO and ACE satellites) carried out by Trotta & Zimbardo ((Trotta and Zimbardo 2011)) shows that the propagation of protons and electrons, can correspond to nondiffusive regimes. The experimental energetic particle fluxes will be compared with the numerical simulation, based on a model derived from the theory of Lévy random walk described below. The thesis is structured in such a way to retrace the research done over the course of the PhD, while respecting their chronology hence the intrinsic relations among the various activities. In this introduction we have framed the context and the problems at the basis of our work by highlighting the objectives and characteristics of the work performed. The second chapter is devoted to issues related to the propagation of Solar Energetic Particles (SEPs) with special reference to the characterization of the events related to the gradual and impulsive phenomena of flares and CMEs and the theoretical apparatus used for their description. The activity was conducted by analyzing a large amount of information available from satellites such as ACE and SOHO in reference to the detection of energetic particles (electrons, protons and ions). In particular, we reported the characteristics of the formalism of propagators as an approach to the solution of the diffusion equation. In the same chapter, there is a selection of pulse events for which the characteristics of the anomalous transport have been shown (superdiffusion). The need to further develop a numerical model for the superdiffusive transport is shown in Chapter 3, in which are shown the characteristics of the turbulent transport in the solar wind combined with the formalization of the paradigm of Levy Random Walk. Starting from the formal description for Levy Random Walk, Chapter 4 is devoted to a description of the numerical

model for the simulation of propagation based on Levy Random Walk with a detailed description of the methodology used, as well as its implementation. The simulation results are shown also in chapter 4, with particular reference to both the determination of the trajectories and the calculation of statistical quantities useful for the validation of the model itself. Furthermore, next chapter describes the approach used for the construction of the transport model of the particles in the solar wind based on a test-particle approach. The conclusions of the work and some consideration on possible future developments are given in Chapter 6.

Chapter 2

The propagation of Solar Energetic Particles

This chapter provides in-depth issues related to the propagation of Solar Energetic Particles (SEPs) based on analysis of data collected by the ACE and SOHO satellites, with particular reference to the classification of gradual and impulsive events, according to the characteristics of the transport of energetic particles themselves. The analysis will focus, then, on impulsive events (typical of the particles emitted by explosive phenomena such as flares). Of particular importance are the theoretical aspects used to describe the transport of energetic particles, the description is carried out by focusing on the characteristics of the statistical approach based on the propagators. The chapter is divided into 3 sections: the first summarizes the characteristics of the classification between impulsive and gradual events, defining the criteria for classifying events as impulsive; the second shows the details of the theoretical approach used for the analysis of the events, i.e. the solution of the diffusion equation through the use of propagators; the third presents the results of data analysis performed on a set of impulsive events for which different types of anomalous transport are recorded (super-diffusive), in relation to the physical characteristics of the particles involved.

The solar corona is a powerful particle accelerator, because it is able to accelerate ions to energies of the order of 1 GeV, and electrons to energies of tens of MeV. These particles escape the coronal plasma and propagate in the solar wind along the spiral magnetic field. Understanding the propagation of energetic particles accelerated at solar flares, coronal mass ejections (CMEs), and interplanetary shocks in the presence of a turbulent magnetic field is one of the main objectives of plasma astrophysics. Indeed the transport properties are crucial for assessing shock acceleration mechanisms (e.g., Duffy et al. 1995; Sandroos and Vainio 2009), for interpreting extreme UV observation of filaments in coronal loops (e.g., Bitane et al. 2010; Galloway et al. 2006) and in coronal hole jets (e.g. Nisticó et al. 2009), and for forecasting the arrival of harmful energetic electrons and protons accelerated near the sun on Earth (Dalla et al. 2003; Ippolito et al. 2005). Because of a background magnetic field B_0, parallel transport and perpendicular transport can have different properties, owing to particle gyromotion, as particles gyrate in the plane perpendicular to the magnetic field and move "freely" along the magnetic field. However, in the presence of magnetic fluctuations, magnetic field lines are distorted, giving rise to a field line random walk (e.g., Shalchi and Kourakis 2007). In addition, resonant wave particle interactions cause pitch-angle diffusion and decoupling of particles from field lines. For the turbulence levels typical of the solar wind, $\delta B/B_0 \sim 0.5$–1, several transport regimes have been considered for the parallel transport of solar energetic particles (SEPs): scatter-free propagation is usually found for electrons (Lin 1974), while proton propagation is often assumed to be diffusive, $\langle \Delta z^2 \rangle = 2D_{||}t$ (e.g., Giacalone and Jokipii 1999; Teufel and Schlickeiser 2002; Zhang et al. 2003). However study of many proton events, based on the onset time analysis, shows that scatter free, i.e. ballistic, transport is also possible for first arriving protons (Dalla et al. 2003; Krucker and Lin 2000). We note that diffusive transport in the direction parallel to the average magnetic field is described by a diffusion coefficient $D_{||}$, and is associated to a parallel mean free path given by $\lambda_{||} = 3D_{||}/v$, where v is the particle speed. The value of $\lambda_{||}$ is very important in the theory of diffusive shock acceleration;

however, its value, even for protons propagating from the Sun to the Earth, is not well known, with estimate that range from about 0.01 AU to several AU (e.g., Chollet et al. 2010; Reames 1999; Teufel and Schlickeiser 2002). The large variability of the inferred values of $\lambda_{||}$ may reflect that diffusive transport is not the only possibility for parallel propagation in the solar wind. In other words, besides diffusive transport and scatter-free (i.e. ballistic) propagation, other transport regimes can be found, in which the particle mean square deviation grows nonlinearly with time, that is, $\langle \Delta z^2 \rangle \sim t^\alpha$.

When $\alpha < 1$, we have subdiffusion, and we have super diffusion when $\alpha > 1$. Recently, Perri and Zimbardo (2009a) have shown that energetic ions accelerated at the solar wind termination shock propagate superdiffusively, with $\langle \Delta z^2 \rangle = 2D_{||}^\alpha t^\alpha$ and $\alpha \simeq 1.3$, with Δz the field line length upstream of the shock. A parallel superdiffusive behaviour is the result of weak pitch-angle diffusion, so that the particle parallel velocity does not change sign very frequently, and very long parallel displacements, called Lévy flights, happen. Weak pitch-angle diffusion can came from low turbulence levels or from the wave particle resonance condition being difficult to satisfy. At the same time, parallel motion is not completely scatter-free, so that an intermediate, superdiffusive transport results. It is interesting to notice that several, independent numerical simulations of particle transport in the presence of magnetic turbulence have shown that, depending on the simulation parameters, perpendicular transport can be subdiffusive (Qin et al. 2002a; Shalchi and Kourakis 2007; Zimbardo et al. 2006), while parallel transport can be superdiffusive (e.g., Pommois et al. 2007; Shalchi and Kourakis 2007; Tautz 2010; Zimbardo et al. 2006). These recent result are therefore at variance with the traditional results of the so-called quasi linear theory (Giacalone and Jokipii 1999; Teufel and Schlickeiser 2002), which predicts normal diffusion both parallel and perpendicular to the average magnetic field. In this chapter we analyse a number of impulsive solar energetic electron and proton events, we study the temporal profile of the particle fluxes in order to determine the transport regime. Different transport regimes are characterized

by different propagators (Perri and Zimbardo 2007; 2008a;b; Ragot and Kirk 1997; Webb et al. 2006), and we show that the observed energetic particle time profiles correspond to quasi-ballistic and superdiffusive regimes.

2.1   Impulsive and gradual events

The right characterization of impulsive events associated with flare and responsible for super-diffusive regimes for the emitted particles was of fundamental importance for the work carried out. In particular, from the work of Reames, 1999 it is possible obtain a very precise characterization of impulsive events in relation to a series of parameters such as the duration and the abundance of certain types of particles. The methodology used in the work of Reames, 1999 starts from the comparison between impulsive events and gradual events, and then it gives a detailed description of the two types of phenomenon. The terminology *impulsive or gradual event* originates from the analysis of X-ray time-scale associated with the event, but now more generally qualifies the different time scales of diffusion of SEP of few MeV. Before describing the typical parameters of an impulsive event, we report the comparison between some characteristics of gradual and impulsive events. This comparative analysis was used in part to select events and, in particular, to isolate the purely impulsive events. The most important parameter comes out from the analysis of trends over time of the particle stream intensity. Figure 2.1 shows the time-intensity charts (variation of flow over time) of protons and electrons in impulsive and gradual events. The fundamental peculiarity of the graphs is that, for the comparison, there have been selected to compare two "pure" events: a CME without flare, and a flare without an associated CME. The gradual event (Figure 2.1(a)) is dominated by protons of about 1 MeV, which form a small peak in the proximity of the passage of the shock. The impulsive event (Figure 2.1(b)) is dominated by electrons, which form a peak by far higher than the gradual phenomenon. The time extension of the gradual event is generated by

the continuous acceleration of the particles by the shock, while the peak of the impulsive event is determined by the scattering of particles that pass through the interplanetary space.
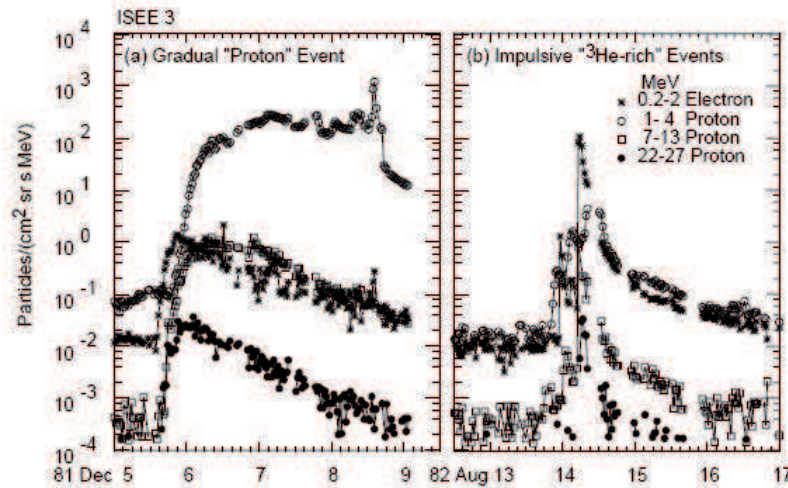

Figure 2.1 Time-intensity Graph for gradual event(a) and impulsive event(b).

Another point of comparison is given by the longitude distribution of gradual events and impulsive events. Figure 2.2 shows the distribution on the longitudes of flare associated to impulsive or gradual events: gradual events are distributed more evenly compared to the solar longitude. The impulsive events are also distributed around the longitude of the best magnetic connection to the viewer. Most of the dispersion in the distribution of the longitude is derived from changes in connection resulting from the speed variation of the solar wind. The remaining dispersion is linked to the random walks of the magnetic field lines that create paths for the particles that connect small portions of the solar surface in distributions till to 1 AU. The width of the distribution for the gradual events suggests the presence of a shock wave which easily propagates through the field lines, and which accelerates the particles along its path.

A further parameter of comparison is linked to the abundance of some isotopes in correspondence of a certain event. Figure 2.3 shows a comparison between the abundances of the various isotopes at about 5 MeV amu-1 in gradual and impulsive events. The higher values of Fe / O are
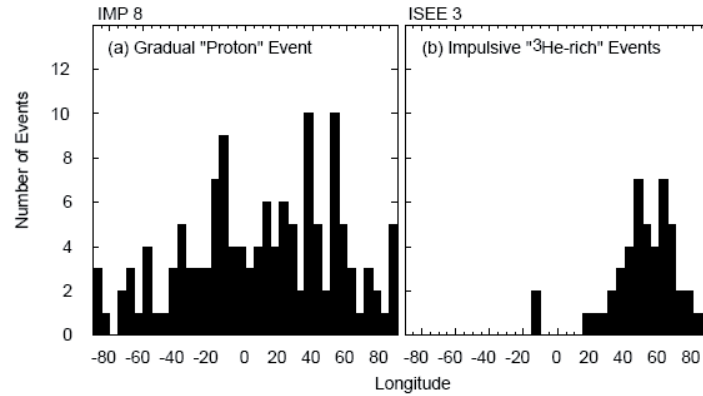
Figure 2.2 Distribution of gradual (a) and impulsive (b) events in relation to the longitude on the solar disk

present in gradual events especially for short time intervals.
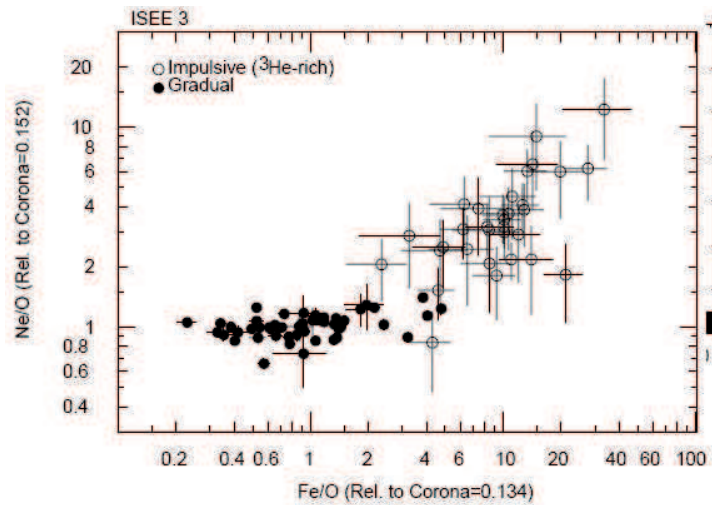
Figure 2.3 Abundances of Fe/O in comparison with Ne/O

A further difference is the abundance of ^{3}He with strongly characterizes impulsive events. The choice to study impulsive events is motivated by the fact that the impulsive events correspond to an injection of particles localized in space and in time, therefore the transport of the particles is described by the shape of the propagator. In other words, the Dirac delta shape of the source

enables the use of the propagator avoiding integration in space and time. The comparison of impulsive and gradual events, help defining, more rigorously, the parameters that characterize the impulsive events. A first characterization can be derived from the study of photons emitted during a solar flare. The emissions of flare are mostly related to thermal emissions of hot plasma or from of non-thermal electrons (i.e. hard X-rays and radio bursts). The observations relating to Îş rays and, in particular, to their temporal profiles, have shown that the ions are actually accelerated also by impulsive flare rather than only from shock waves. In a study of Cliver et al. (1989) has been made a comparison between events SEP and X-rays from the flare in a period of 5 years in the vicinity of the maximum solar activity. In this context, a number of projects have been carried out to show the strong connection between impulsive events, such as flares, and the abundant presence of ^3He particles. In particular (Mandzhavidze et al. (1999) and Share and Murphy (1998)), the comparative analysis between the lines produced by ^4He and ^3He with the γ rays emitted in the bombardment with ^3He of He, O and Fe and in particular with lines to 0.957 MeV dropout of ^{18}F through ^{16}O, it was noticed that in 7 flare, on the 20 examined, the ratio $^3He/^4He > 0.1$ and in some cases the ratio $^3He/^4He \sim 1$. Furthermore, the authors stressed the independence of the phenomenon of the flare duration, making it even more evident that impulsive events (flare) in the low corona are ^{3}He-rich events. The measurements made by the satellite ISEE-3 have shown the connection between events rich in ^3He with the presence of non-relativistic scatter-free electron beams (10 - 100 keV) that generate radio burst of type III. The dispersion of the velocity of the particles is consistent for electrons and ions (the particles are detected in reverse chronological order with respect to their speed). This can be used to determine the initial standing on the sun of the accelerated particles in a few minutes. The association between the stream of electrons and the radio bursts of type III (of the order of both meter and kilometer) coincides with the time necessary for the association with the flare H_α and X-rays. Immediately after the discovery of the events rich in ^3He associated to the flare, hence to impulsive events, it has been discovered that in these events

is unusual the presence of elements other than Fe. In the analysis of our events, all the parameters described above were taken into account in such a way as to identify precisely the events purely impulsive to be used for the study of the diffusion of energetic particles.

2.2   Diffusion equation and propagators

The method that we use is based on the propagator formalism. The propagator $P(\vec{r} - \vec{r'}, t - t')$ is the probability density function that a particle injected in $\vec{r'}$ at time t' is found in $\vec{r}$ at time t, and is obtained as the solution of the appropriate transport equation for the sharp initial conditions $P(\vec{r}, t = 0) = \delta(\vec{r})\delta(t)$ (e.g., Metzler and Klafter 2000). For the case of particles injected in a homogeneous system at different positions and times, the number density $n(\vec{r}, t)$ can be obtained as

$$n(\vec{r}, t) = \int P(\vec{r} - \vec{r'}, t - t')q(\vec{r'}, t')d^3r'dt' \tag{2.1}$$

where $q(\vec{r'}, t')$ is the particle number density per unit time at the injection places and times. We can assume that for each given energy E the flux of particles is proportional to the number density of particles with that energy. The propagator describes the transport properties, and it can be seen that for different transport models and different particle injections at the source, a wide variety of particle densities at the observer in $\vec{r}$ can be obtained as a function of time. Let us consider a few limiting cases.

Sharp localized injection at the origin: in such a case $q(\vec{r'}, t') = A\delta(\vec{r'})\delta(t')$, where A is a normalization constant with appropriate physical dimensions, and the integration of Eq. (1) immediately yields

$$n(\vec{r}, t) = AP(\vec{r}, t) \tag{2.2}$$

in agreement with the fact that the propagator is the solution of the transport equation for δ-function initial conditions.

Ballistic propagation: in such a case, particles move freely away from the source at a constant speed. We consider the one-dimensional (1D) case for clarity, so that the propagator is given by Webb et al. (2006)

$$P(z-z',t-t') = \frac{1}{2}[\delta(z-z'-v(t-t')) + \delta(z-z'+v(t-t'))], \tag{2.3}$$

where the δ functions describe the propagation at constant speed in the two opposite directions. Considering a particle injection localized in space but not in time, $q(z',t') = A\delta(z')f(t')$, and inserting the above expression into Eq. (1), we obtain upon integration over z'

$$n(z,t) = \frac{A}{2}\int[\delta(z-v(t-t')) + \delta(z+v(t-t'))]f(t')dt' \tag{2.4}$$

whence, assuming that the observer is at $z > 0$,

$$n(z,t) = \frac{A}{2|v|}f(t-\frac{z}{v}). \tag{2.5}$$

(For $t > t'$, $v > 0$ the second δ function is always zero). It can be seen that, for ballistic propagation, the time profile of particle emission at the source is translated to the observer in z undistorted and backshifted in time by a lag z/v—the time of flight. If, on the other hand, the transport is not purely ballistic, the time profile at emission $f(t')$ will be modified by propagation (for instance, it will be smoothed).

Particle emission at a traveling planar shock: we assume that the observer–shock distance is much less than the size of the shock, as in the case of interplanetary shocks. In such a case the particle source can be assumed to be an infinite plane, say the xy plane, which moves along the z direction with velocity V_{sh}. The problem is then 1D, and the source of particles can be described as $q(z',t') = A\delta(z' - V_{sh}t')$, so that the particle number density at the observer will be

$$n(z,t) = A\int P(z-z',t-t')\delta(z'-V_{sh}t')dz'dt'. \tag{2.6}$$

This is the case considered by Perri and Zimbardo (2007; 2008a) for analysis of energetic particles accelerated at corotating interaction region (CIR) shocks, where the scale size of the CIR

shock, about 5–10 AU, is much greater than the spacecraft-CIR distance, below 1 AU for the considered shocks. Perri and Zimbardo (2007; 2008a) used the above expression to show that, if a Gaussian propagator is assumed, corresponding to normal diffusion, an exponential profile $\exp(-V_{sh}z/D)$ is obtained for the accelerated particle fluxes, in agreement with the classical view (e.g., Lee and Fisk 1982). Conversely, if a power-law propagator is assumed, corresponding to superdiffusion, a power-law particle profile is obtained.

In the following, we analyse the observed particle profiles for a number of SEP events. The particle time profiles are fitted by power laws: considering propagators with asymptotic time profiles, the transport regime for the particles is determined from the fit. To proceed, we make the following assumptions:

1. localized injection of energetic particles, described by $\delta(\vec{r})\delta(t)$, so that Eq. (2) holds. In such a case, the observed particle profile corresponds to the propagator. This restricts our analysis to impulsive SEP events, where energetic particles are injected at once in a localized region, probably by a flare.

2. No multiple injections of energetic particles for the same event. This requires a careful selection of the analysed events.

3. Normal perpendicular transport, i.e., diffusive, so that the propagator for perpendicular transport has the well known Gaussian form. Therefore, we only investigate the possibility of anomalous transport for propagation along the magnetic field.

We now consider a localized injection of energetic particles at time $t' = 0$ and position $\vec{r'} = (0,0,0)$. The transport properties can be described by the probability $P(\vec{r},t)$ of observing the injected particles at $\vec{r} = (x,y,z)$ at time t. For normal diffusion in the presence of a magnetic field,

this can be written as (e.g., Metzler and Klafter 2000; Ragot and Kirk 1997; Webb et al. 2006)

$$P(\vec{r},t) = \frac{N_0}{(4\pi t)^{3/2}\sqrt{D_\perp^2 D_\parallel}} \exp\left[-\frac{x^2+y^2}{4D_\perp t} - \frac{z^2}{4D_\parallel t}\right] \tag{2.7}$$

where N_0 is the total number of injected particles, while $D_\perp$ and $D_\parallel$ represent the diffusion coefficients perpendicular and parallel to the average magnetic field $\vec{B}_0$, respectively, with $\vec{B}_0 = B_0\hat{e}_z$. For magnetic turbulence levels $\delta B/B_0 \sim 0.5$–1.0, typical of the solar wind, $D_\parallel$ is usually much larger than $D_\perp$ (Giacalone and Jokipii 1999; Pommois et al. 2007). In what follows, we will select impulsive SEP events, which approximate the localized injection well at the origin of coordinates. In such a case the observed particle flux is proportional to the propagator, which describes the space-time distribution of the particles injected at the origin of space and time. In our analysis, we consider the observed particle fluxes for late times, that is, for times such that the absolute value of the argument of the exponential functions in Eq. 2.7 is much less then 1 , e.g. $z^2/4D_\parallel t << 1$. In such a case, the exponential functions tend to $lim_{x\to 0}\exp[-x^2] = 1$, and the long time behaviour of the particle flux is given by the factor

$$\frac{N_0}{(4\pi t)^{3/2}\sqrt{D_\perp^2 D_\parallel}}. \tag{2.8}$$

Therefore, a power law decay of the energetic particle time profile proportional to $t^{-3/2}$ is indicative of normal Gaussian diffusion.

On the other hand, in the case of anomalous, superdiffusive transport, the propagator can be obtained in the framework of continuous time random walks (Friedrich et al. 2006; Klafter et al. 1987; Zumofen and Klafter 1993) in Fourier-Laplace space. Superdiffusion is characterized by a space-time, coupled probability of jumps by the random walker of the form $\psi(l,\tau) = Cl^{-\mu}\delta(l - v\tau)$, which is valid for large l, where l is the jump length, v the walker velocity, and τ the jump time. Such a probability defines a Levy random walk whose distinctive property is a power-law distribution of jump lengths with exponent μ (Klafter et al. 1987), and should not be confused with

the propagator itself. The power-law distribution of jump (i.e., free displacement) lengths means that long jumps have a small but non-negligible probability. These long jumps make transport faster than normal, and long jumps are frequent enough for $2 < \mu < 3$ to enforce superdiffusion. It is important to notice that the mean square value of l is diverging for $\mu < 3$, so that no mean free path can be defined, and the central limit theorem, which would imply normal diffusion, does not apply. The power-law distribution of jump lengths in the Lévy random walk implies (by means of a proper statistical treatment) a power-law probability density function for the random walker position, or, in other words, a propagator with power law tails (Zumofen and Klafter 1993). For a full discussion, see the reviews by Bouchaud and Georges (1990); Metzler and Klafter (2000; 2004). Therefore, while normal diffusion is related to a Gaussian propagator and, usually, a Gaussian distribution of jump lengths, which corresponds to Brownian motion, anomalous diffusion is related to propagators and distribution of jump lengths having power-law tails.

We then consider superdiffusion along the z direction, which is the direction of the average magnetic field, while perpendicular transport here is assumed to be normal. In a few limiting cases, the Fourier-Laplace transform of the propagator can be inverted

1. for long times (near the source), that is for $|z| \ll k_\mu^{\frac{1}{2}} t^{1/(\mu-1)}$, we have

$$P(z,t) = a_0 t^{1/(1-\mu)} \exp\left[-\frac{z^2}{k_\mu t^{2/(\mu-1)}}\right]; \qquad (2.9)$$

2. for short times (far from the source), that is for $|z| \gg k_\mu^{\frac{1}{2}} t^{1/(\mu-1)}$, we have for $z < vt$

$$P(z,t) = b\frac{t}{z^\mu}, \qquad (2.10)$$

and $P(z,t) = 0$ for $z > vt$, where a_0, b, and μ are constants and k_μ is an anomalous diffusion constant (Zumofen and Klafter 1993). The value of μ determines the type of transport: superdiffusion is obtained for $2 < \mu < 3$, transport is diffusive for $3 < \mu < 4$ even if the propagator is non-Gaussian but a power law, and transport is ballistic (i.e. scatter-free) for $1 < \mu < 2$ (Zumofen and Klafter

1993). Superballistic regimes can also be obtained, see Klafter et al. (1987) and Zimbardo et al. (2000b). For $2 < \mu < 3$, the following diffusion law is valid:

$$\langle \Delta z^2(t) \rangle = 2D_\alpha t^\alpha \tag{2.11}$$

where the exponent of anomalous diffusion α is related to the exponent μ in the propagator by $\alpha = 4 - \mu$. In our analysis of impulsive SEP events, the propagator form related to superdiffusive transport is used, in particular, its form calculated in real space in the approximation of long times (i.e. $| z | \ll k_\mu^{\frac{1}{2}} t^{1/(\mu-1)}$). In such a case the exponential term of (2.9) stretches to 1, and the propagator assumes the form

$$P(z,t) \sim \frac{a_0}{t^{1/(\mu-1)}}. \tag{2.12}$$

We note that the comparison between power-law propagators and tracer particle distributions is also used in laboratory plasmas to determine the transport regimes (del-Castillo-Negrete et al. 2004).

We now make the assumption that perpendicular transport is normal in most cases: although subdiffusive and sometimes superdiffusive transport have been found for perpendicular transport (Qin et al. 2002a; Shalchi and Kourakis 2007; Zimbardo 2005; Zimbardo et al. 2006), numerical simulations show that perpendicular transport is normal in most cases of strong turbulence (Pommois et al. 2007; Tautz 2010). In particular, Qin et al. (2002a) show that perpendicular subdiffusion is obtained in the case of a prevailing slab turbulence, while Qin et al. (2002b) show that normal diffusion is recovered in the case of prevailing two dimensional turbulence, as may occurs in the solar wind. Also, perpendicular subdiffusion is usually the result of particles tracing back the magnetic field lines, a phenomenon called compound diffusion; however, this does not happen if enough field line stochasticity is present. Recently Zimbardo et al. (2009) and Bitane et al. (2010) have shown that field line stochasticity grows with the quasi-2D anisotropy and that perpendicular transport is usually diffusive in space plasmas. Therefore, we assume that, even in the case of parallel superdiffusion, perpendicular diffusion is described by the Gaussian propagator, that the

3-D propagator is the product of the propagators for perpendicular transport $P_\perp(x,y,t)$ and that for parallel transport $P_\parallel(z,t)$

$$P(\vec{r},t) = P_\perp(x,y,t) \times P_\parallel(z,t). \tag{2.13}$$

We notice that this expression implies that the probabilty for perpendicular transport is independent of the probability for parallel transport; this may not be the case in a magnetized plasma due to compound diffusion, (see, Webb et al. 2006; Zimbardo 2005; Zimbardo et al. 2009). However, once the transport regime is known, the probability of being at a given position can be described in the same way as above, the probability being a statistical quantity. More in detail, we have

$$P(\vec{r},t) = \frac{N_0}{4\pi t D_\perp} \exp\left[-\frac{x^2+y^2}{4D_\perp t}\right] \times \frac{a_0}{t^{1/(\mu-1)}} \exp\left[-\frac{z^2}{k_\mu t^{2/(\mu-1)}}\right]. \tag{2.14}$$

Again considering the limit for long times, we are left with

$$P(\vec{r},t) \simeq \frac{N_0 a_0}{4\pi D_\perp t^{1+(1/(\mu-1))}} \sim \frac{1}{t^{\mu/(\mu-1)}} = t^{-m} \tag{2.15}$$

where $m = \mu/(\mu-1)$. We have super diffusion for $2 < \mu < 3$, while ballistic regimes where $\langle(\Delta z)^2\rangle \sim v^2 t^2$ are found for $\mu < 2$ (Zumofen and Klafter 1993), and normal diffusion is found for $\mu > 3$. Therefore, the slope of the particle flux decay for long times should be $m = 3/2$ for normal diffusion, $m = 2$ for nearly ballistic transport, and $3/2 < m < 2$ for superdiffusive transport. In other words, a slope of the particles flux decay greater than $3/2$ is indicative of either superdiffusive or ballistic transport. Also, for $3/2 \leq m \leq 2$, we obtain $\mu = m/(m-1)$, and the anomalous diffusion exponent is $\alpha = 4 - m/(m-1)$.

We note that, in the case of strictly ballistic transport, the propagator is given in terms of delta functions, as seen in the Introduction. However, Zumofen and Klafter (1993) have shown that anomalous quasi-ballistic transport with some scattering, which may correspond more closely to the observed scatter-free events, may also be described in terms of CTRW, provided the exponent μ in the jump probability $\psi(l,\tau) = Cl^{-\mu}\delta(l-v\tau)$ satisfies $1 < \mu < 2$. In such a case, particles are moving back and forth, but long free displacement have such a high probability that $\langle(\Delta z)^2\rangle \sim v^2 t^2$

results (Klafter et al. 1987; Zumofen and Klafter 1993). For $1 < \mu < 2$, the analytical inversion of the Fourier-Laplace transform is not known in general; that is, Eq. (2.9 - 2.10) do not hold. However, we suggest that, when $m = \mu/(\mu - 1) > 2$, this may correspond to $\mu < 2$, that is, to quasi-ballistic transport, which, including some scattering, may be a more realistic and complete description of scatter-free events. In particular, (Perri and Zimbardo 2008b) suggest that the spike in the propagator obtained for $\mu = 3/2$ corresponds to the observed electron profiles for scatter-free events. Finally, other forms of the propagator for non Gaussian transport have been given by Ragot and Kirk (1997) and by Webb et al. (2006)..

2.3 Impulsive events selection

All the dataset we consider were obtained from the CDAWeb service of the National Space Science Data Center (cdaweb.gsfc.nasa.gov). The selection of the events starts with identifying those periods with no influence on transient events like CMEs, so that the background conditions remained relatively unperturbed and the event profiles are very well defined and easily recognized.

The characterization of the impulsive events follows the criteria proposed by Reames (1999): intensity-time profiles of electrons and protons with a prevalence of electron intensity and a duration of tens of hours. Besides this, they are ^{3}He-rich events. Normally impulsive events came from a flare (or a series of flares) without associated CME (*pure event*). Event selection starts from examining electron fluxes from ACE/EPAM datasets. Events that exhibit a characteristic intensity-time profile, i.e. fast rise and smooth decay, were selected for ^{3}He analysis. The ^{3}He data are from ACE/ULEIS (Ultra Low Energy Isotope Spectrometer) instrument and are related to the same time interval of the chosen event: only ^{3}He-rich event were chosen. Impulsive SEPs event are also characterize by the short $[< 1hr]$ duration of the associated soft X-ray (SXR) burst. To test the SXR burst duration we inspected data from the GOES-8 Space Environment Monitor for the same time

Data	E_{max}	Satellite	t_0	t_1	t_{max}	m	α	μ	χ^2	Flare-coords
	MeV		*h*	*h*	*h*	*h*				
2000 June 10										
Protons	16.40	SoHO	17:00	1.00	2.00	2.09	2.00	1.92	0.20	N22W38
	33.00	SoHO	17:00	2.00	2.00	2.19	2.00	1.84	0.22	
Electrons	0.05	ACE	17.00	1,00	1,00	1.56	1.22	2.78	0.36	N22W38
	0.10	ACE	17.00	1.00	1.00	1.69	1.56	2.44	0.24	
	0.18	ACE	17.00	1.00	1.00	1.76	1.69	2.31	0.12	
	0.32	ACE	17.00	1.00	1.00	1.79	1.73	2.27	0.09	
2001 July 19										
Electrons	0.05	ACE	4:00	5.00	10.00	1.74	1.64	2.36	0.08	N13W72
	0.10	ACE	4:00	5.00	10.00	1.72	1.61	2.39	0.02	
	0.18	ACE	4:00	5.00	10.00	1.61	1.36	2.64	0.01	
	0.32	ACE	4:00	5.00	10.00	1.23	1.00	-	0.03	
2002 Feb 20										
Protons	0.112	ACE	5.55	2.00	18.00	1.30	1.00	-	0.28	N12W72
	0.187	ACE	5.55	2.00	18.00	1.11	1.00	-	0.15	
	0.310	ACE	5.55	2.00	18.00	0.99	1.00	-	0.08	
	0.580	ACE	5.55	2.00	18.00	0.97	1.00	-	0.05	
Electrons	0.05	ACE	5.55	1.00	2.00	1.97	1.97	2.03	0.09	N12W72
	0.10	ACE	5.55	1.00	2.00	2.12	2.00	1.89	0.07	
	0.18	ACE	5.55	1.00	2.00	2.16	2.00	1.87	0.04	
	0.32	ACE	5.55	1.00	2.00	2.03	2.00	1.97	0.03	

Table 2.1 Main parameters of selected event. E_{max} is the maximum value of the energy channel. The columns t_0, t_1, and t_{max} are the start time in corona, the time delay from start to instrument detector, and time delay from start to of particle-flux maximum. The columns m, μ, and α are related to the transport regime, see text. The column χ^2 shows the value of the χ^2 test for m fit.

interval. We analysed the time profile in the long time approximation looking for those events that exhibit a superdiffusive (ballistic) appearance either for proton and/or for electron flux.

To analyse the characteristic of intensity-time profiles (e.g. the diffusion properties), we inspected each event to determine the origin in the corona, i.e. the start time of the event. To do that we looked for a type III radio burst related to impulsive SEPs event. Type III radio burst data are from WIND Waves RAD2. The occurrence of radio type III bursts, starting in the corona and traveling into interplanetary space, are related to the flare-accelerated electrons at the origin of the event. The analysis was made using 10 minute averages and time-intensity graphics. Assuming that the spacecraft is connected well to the flare site, the event's start time coincides with the type III onset time (e.g. the electron release coincides with radio type III burst (see also Krucker and Lin (2000)).

Many studies have focused on the role of the heliographic longitude of the source by analyzing SEPs data from near-earth spacecraft (Dalla et al. 2003; Ippolito et al. 2005; Krucker and Lin 2000; Reames 1999). Those studies find that impulsive SEPs event can be observed when the source region is in the *well-connected* longitudinal range (that is, from W20 to W90). The positional data of the flare (e.g. coordinates) associated to the event is compared with intervals in the *well-connected* longitudinal range. The flare data are from National Geophysical Data Center (NGDC) solar data. Among the many events that have been identified we report here three events that serve to exemplify the different transport regimes. The event characteristics and the obtained transport regimes are given in Table 2.1.

2000 June 10

The 2000 June 10 impulsive event is shown in Fig. 2.4. This is associated with an M 5.2 class GOES flare at heliographic position N22W38. In the left column of Figure 2.4 from top to bottom are shown, on a lin-log scale, the proton fluxes measured by SoHO in the energy chan-
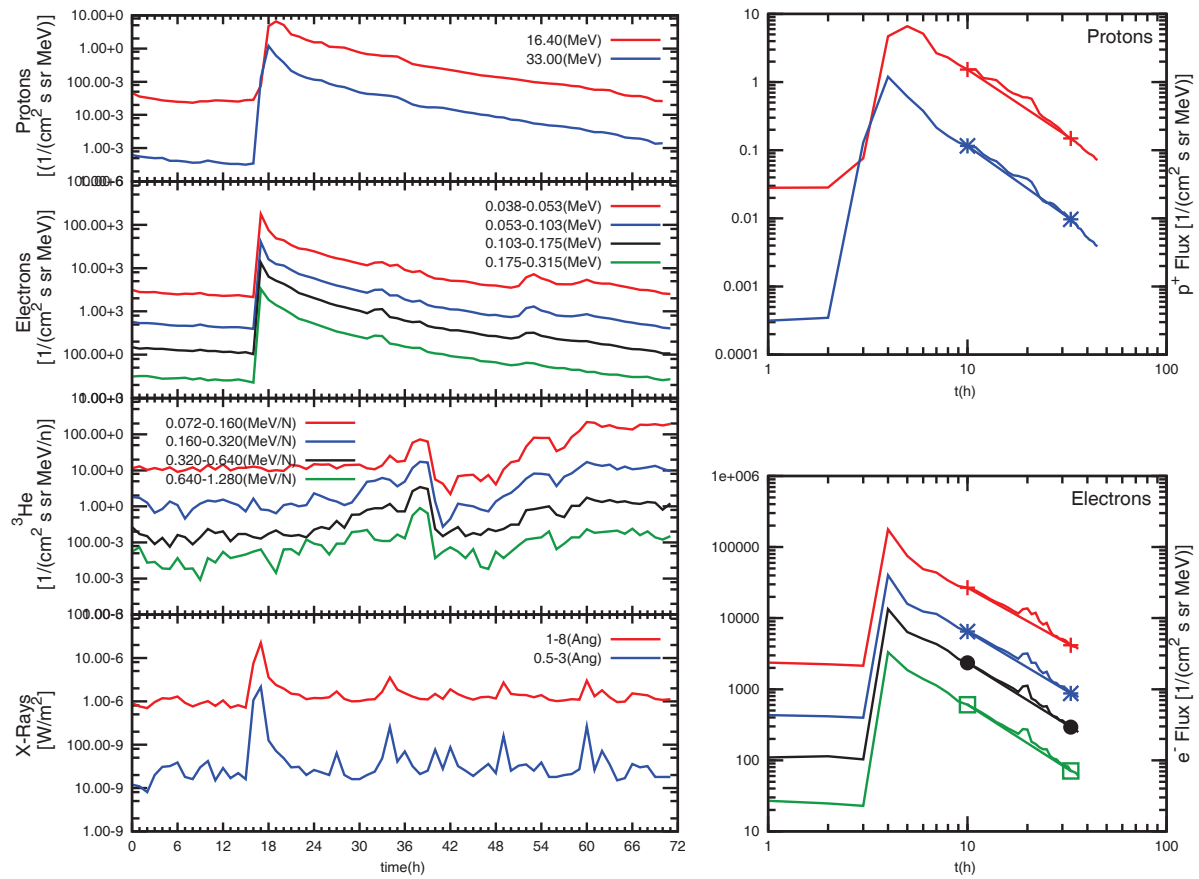
Figure 2.4 2000 June 10 impulsive event. On the left: lin-log graph of fluxes data; from top to bottom: proton flux from SoHO, electron flux from ACE/EPAM, ^{3}He flux from ACE/ULEIS and X-rays from GOES/SEM. On the right: electron and proton log-log graph with linear fit in the descending zone.

nels 16.4 MeV and 33.0 MeV, the electron flux from ACE/EPAM in the energy channels 0.038-0.053Mev, 0.053-0.103MeV, 0.103-0.175MeV, 0.175-0.315MeV, and the ^{3}He fluxes measured by ACE/ULEIS in the energy channels 0.072-0.160MeV, 0.160-0.320MeV, 0.320-0.640MeV, 0.640-1.280MeV, and the X-Rays flux from GOES/SEM in the wavelengths 1-8 Å(HXR) and 0.5-3 Å(SXR). In the graphs, the data are averaged hourly and are synchronized with the start time at the source. The ^{3}He peak is delayed $\sim$ 20h owing to the lower ^{3}He speed. Indeed, considering the speed as a function of energy and mass of particles and assuming that the distance traveled along the magnetic field spiral is about 1.2 AU (e.g., Krucker and Lin 2000), we find that the ^{3}He flux should be shifted at least 15 hours with respect to the proton. The flare is shown by the peak present in X-rays, and is highly synchronized with the peak flux of protons and electrons. All this properties indicate that this is an impulsive event. The event start time is determined by analyzing radio type III burst in order to determine the origin of the time axis, as explained above.

The proton and electron fluxes suddenly rise simultaneously because we are using hourly averages, thus loosing the evidence of velocity dispersion for electrons of different energies (e.g., Lin 1974; 2005). At the same time, the spiky profiles themselves indicate a fast, nearly scatter-free propagation and a good magnetic connection with the acceleration site. The characteristics of the transport of SEPs are linked to form of the propagator during the decay phase, as explained in Sect. 2. To determine the power-law scaling of the energetic particle fluxes, we plot them on log-log axes (Figures 2.4, right panels). The origin of the time axis is determined using the event start time, and the linear fit was performed on the decay phase of the event. To respect the condition that the propagator form for long times is valid, we fit the flux starting at about ten hours after the event start time, that is, well after the peak in the particle fluxes. The electron and proton graphs (Fig. (2.4) are on a time range of $\sim$ 50 hours for all energy channels. The onset time (origin) was set to 2000 June 6 at 17:00. The peak of the event is seen at $\sim$ 4 hours from the origin. The fit was made on 25 points after $\sim$ 10 hours from the event's start time.

The quality of the fit was evaluated using the χ^2 test which shows that the fit is usually very good. Also, visual inspection of time profiles in the right hand panels of Figure 2.4 shows that the particle flux decay is represented well by power laws. The power-law index is given by $m = \mu/(\mu - 1)$, see Eq. (2.15). The slope (reported in Table 2.1) and the calculation of the exponent μ indicate superdiffusive transport with $\alpha = 1.56 - 1.79$ for electron, ballistic (e.g. scatter-free) transport, $\alpha \sim 2$ for protons. This type of transport is consistent with the rapid rise and decay in the energetic particles profile, typical of scatter-free events (e.g. Lin (1974))
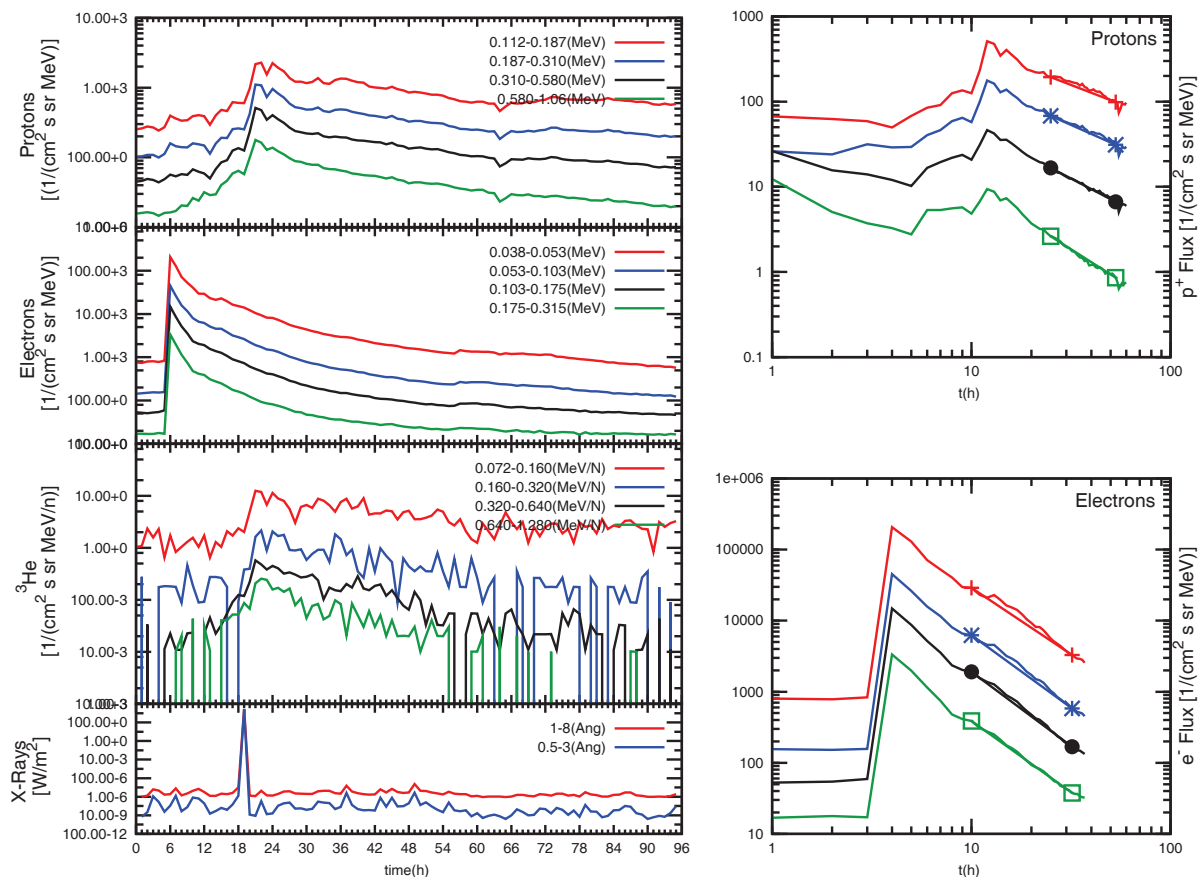
2002 February 20

Figure 2.5 Same as Figure (2.4), but for the 2002 February 20 impulsive event.

This event, shown in Figure 2.5, is characterized by different transport regimes for protons and electrons. As above, proton and electron fluxes are compared with ^{3}He flux and SXR to characterize the event as an impulsive event. The 2002 February 20 impulsive event is associated with an M 5.1 class GOES flare at heliographic position N12W72. The prompt arrival of the electrons shows that a good magnetic connection between the spacecraft and the acceleration site is present. The start time t_0 has been set 2002 February 20 at 5:55. The peak of the event is seen at ~ 1 h from t_0 for electrons and ~ 18 h from t_0 for protons. This long delay of the proton maximum is due to the lower proton energies measured by ACE, 0.11 - 1.06 MeV, compared to those of SoHO in Figure 2.5, 16.0 - 33.0 MeV. As with the previous event, to determine the power-law scaling of the energetic particle fluxes, we plot them in log-log axes (Fig. 2.5). The origin of the time axis is determined using the event start time, and the linear fit was performed on the decay of the event excluding the peak, but starting the fit at 20 h delay for protons and at 10 h for electrons.

The quality of the fit was evaluated using the χ^2 test. The electrons and protons (Figure 2.5 on the left) profiles have different time ranges: ~ 52 h for all energies channels of electrons and ~ 72 h for all energies channels of protons.

Because of the different intensity-time profiles between electrons and protons, the parameters of fit were different in a number of features. The slopes of the particle profile are reported in Table 2.1. For protons we find $m = 0.97 - 1.3$, that is, values lower than 3/2, so that normal diffusion is obtained for protons in this event. We recall that the relation $\mu = m/(m-1)$ only holds for $3/2 < m < 2$, so that the value of μ is not given in this case in Table 2.1. Conversely, for electrons $m = 1.97 - 2.16$, that is, the value nearly equal to two or larger than two. This implies ballistic or quasi-ballistic transport, i.e., $\alpha = 2$. We note that such a ballistic regime is consistent with the scatter-free electron propagation considered by Lin (1974; 2005), and the very spiky electron profiles of this event are not very different from those considered by Lin (1974; 2005). However, introduction of the propagators corresponding to superdiffusive transport or to quasi-ballistic transport allows the

decaying part of the electron profile to be interpreted as the result of scattering of a limited number of particles and not as the effect of continued electron acceleration at the source.
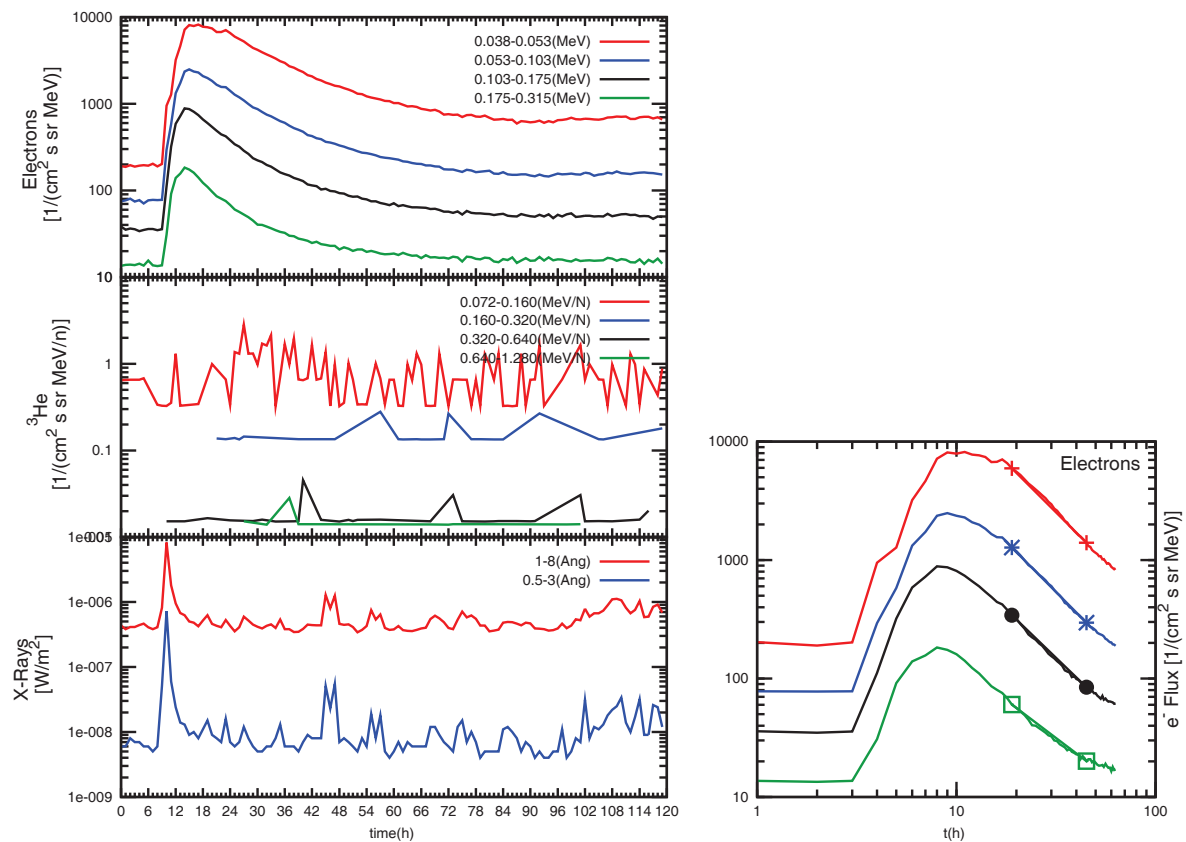
2001 July 19

Figure 2.6 2001 July 19 impulsive event. On the left: lin-log graph of fluxes data; from top to bottom: proton flux from ACE/EPAM, ^{3}He flux from ACE/ULEIS and X-Rays from GOES/SEM. On the right: Electrons log-log graph with linear fit in descending zone.

Unlike the previous events, for the 2001 July 19 event we did not analyse protons because the data relative to proton fluxes were very disturbed. The event is shown in Figure 2.6 where electron fluxes are compared with ^{3}He flux and SXR. The 2001 July 19 event is associated with a flare at

heliographic position N13W72. From top to bottom are shown on lin-log scale the electron flux from ACE/EPAM in the energy channels 0.038-0.053 MeV, 0.053-0.103 MeV, 0.103-0.175 MeV, 0.175-0.315 MeV, and the ^{3}He fluxes measured by ACE/ULEIS in the energy channels 0.072-0.160 MeV, 0.160-0.320 MeV, 0.320-0.640 MeV, 0.640-1.280 MeV. The bottom panel shows the X-ray flux from GOES/SEM in the energy channels 1-8 Å(HXR) and 0.5-3 Å(SXR). That the magnetic connection was not good is also indicated by the electron profiles not being sharply peaked, suggesting that some cross field propagation was necessary before the electron flux maxima were reached. The flare is shown by the peak present in X-rays, and it happened about 5 h before the electron flux maxima.

As for the previous events, we made the power-law fit on the decay phase of the profiles, as indicated in the right panel of Figure 2.6. To minimize the influence of cross field diffusion on the electron profile, we started to fit at 20 h after the start of the event. The power-law exponents (reported in Table 2.1) and the calculation of the exponent μ indicate superdiffusive transport for electrons with energies from 0.05 MeV to 0.18 MeV, with anomalous diffusion exponent $\alpha = 1.36 - 1.64$. On the other hand, normal diffusion is found for an electron energy of 0.175-0.315 MeV, see Table 2.1. For this event, we notice that the α decreases with increasing energy. However, for the event of 2000 June 10, it is found that α increases with energy, so that a clear trend of the anomalous diffusion exponent with energy cannot be identified at this stage.

Chapter 3

Lévy Random Walk approach to problem of transport

This chapter reports the motivation and the properties of the numerical model for the analysis of superdiffusive transport based on Lévy Random Walk. In particular, starting from the definition of the problems related to the transport of particles for non-impulsive events (generated by phenomena such as CME), the emphasis is on the need to build models for the study of superdiffusive transport, in order to compare the theoretical results with the characteristics of the observed data. The chapter also discusses in-depth issues related to both the characteristics of parallel and perpendicular transport and the theory of Levy random walk. The objective of this approach is, therefore, the ability to "describe" regimes of anomalous transport using precisely the theory of Lévy walks. Through the numerical simulation it is possible to show the different characteristics of non-Gaussian distributions. The chapter is structured as follows: the first section describes the characterization of the issues related to transport in gradual events for which it is necessary the use of numerical models for the study of super-diffusive transport; in the second section we examine the motivations and the difficulties for the construction of a numerical model for the super-diffusive

transport; the third section highlights the characteristics of the parallel and perpendicular transport with particular reference to the motion of particles in the solar wind; in the fourth and last section we describe the theoretical aspects related to Lévy Random Walk.

As reported in previous chapter, in recent years, the study of transport phenomena linked to phenomena such as CME and flare has been much developed. In particular, the study focused on the analysis of the temporal profiles of the flows of electrons and ions associated with these events (Cane et al, 1988; Reames, 1999; Trotta and Zimbardo, 2011). The particles involved in this kind of phenomena (that can reach energies up to 1 GeV), can reach distances that exceed 1 AU. The SEP phenomena of long duration (several days) are classified as gradual events. The gradual events observed are often associated with the CME that, also by virtue of the interaction with the interplanetary magnetic field, expands moving outward. The interaction of the particles with the solar wind turbulence in front of the CME determines the characteristics of the transport itself. There are several theoretical works related to the study of the motion of these particles and their transport characteristics (Lee, 1983, 2005; Reames, 1999; Giacalone and Kota 2006).

In particular, these studies deal with the motion of particles through a given magnetic field with fluctuations linked to phenomena of turbulence with a certain degree of correlation. The construction of "realistic" models for gradual SEP events are the challenge for simulations of space weather because of their fundamental importance in predicting the risk intrinsically linked to events of this kind. There are several numerical models for the study of shock and consequent phenomena of particle acceleration aimed at the study of the temporal profiles associated with SEP (e.g. Cane et al.,1998; Vainio et al. 2006). All these models use different types of simplifying assumptions in order to make the problem tractable from the mathematical and / or computational point of view. In general, the problem of modeling a gradual event represent a strong challenge (currently unresolved) because of the time and space variability of the acceleration source, i.e., the shock, and of the variety of possible transport regimes.

A useful approach to the study of these phenomena could be based on the properties of Lévy random walk to be used for the study of transport characteristics in gradual events: having set the model to use for the description of the shocks associated with CMEs, the properties of motion of the particles through the shock can be modeled using, in fact, the Lévy Random Walk.

3.1 Lévy Random Walk

The diffusive processes are fundamental in the description of conservative and dissipative chaotic systems, which is why they have a fundamental importance in many applications of various scientific fields other than physics: the theory of diffusion is used, for example, in geology, economics and the social sciences. Over the years, several paradigms have been proposed for the study of diffusion problems, based on different formalisms. For our work we have used models based on Lévy Walks, i.e. statistical descriptions that "extend" the concepts related to the formalization of the random walks. In particular we emphasize the difference between Lévy Fligth and Lévy Walk, both mathematical models used to describe the anomalous diffusion, characterized by having standard deviations not linearly related to time. The flight follow the Lévy probability distributions $P[R]$, whose average standard deviation is infinitive, with a non-zero probability of very long jumps irrespective of the time needed to perform the jump. The Lévy Walk, instead, has a coupling space-time which penalizes very long jumps. In other words, for Lévy Walks we assume that a proportion ally longer time is needed to make long jumps. The models are called Lévy models in honor of the mathematician Paul Lévy who, in the years between 1920 and 1930, developed the mathematics on statistics of the motions with infinite standard deviation. As mentioned in the previous paragraphs, the observation and description of diffusion processes based on the random walk goes back in time. In 1700 J.Bernoulli (Ars Cojectandi) describes the random "paths" related to the mechanisms of gambling, although the best known example is definitely the

description of the irregular motion of particles described by R. Brown in 1800. The revolutionary bit of Brown's work was the demonstration that this type of movement is independent from the origin of the particles and it is not caused by differences in temperature or pressure. The formalism of the Lévy Walk is particularly suitable for the description of phenomena called *superdiffusive*, and it also has characteristics of self-similarity and invariance of scale factors typical of fractal geometry (Metzler and Klafter 2000; 2004).

3.1.1 Diffusion

There are different "types" of diffusion classified according to the relationship between the standard deviation and the time. The simplest diffusion process is the Brownian motion whose mean square displacement is given by:

$$\langle \vec{r}^2(t) \rangle \sim 2Dt \tag{3.1}$$

where $\vec{r}^2(t) = (x - x_0)^2 + (y - y_0)^2 + (z - z_0)^2$. In his category of movements, the probability distribution is given by a Gaussian according to the central limit theorem (Shlesinger et al. 1993). In the case of anomalous transport, the relationship between the mean square displacement and the time is no longer linear, for which the diffusion equation becomes (Klafter et al. 1990)

$$\langle \vec{r}^2(t) \rangle \sim t^\alpha \tag{3.2}$$

The exponent α distinguishes between two different types of diffusion: if $\alpha < 1$ we have subdiffusive processes (Klafter et al. 1990); if $\alpha > 1$ we will have super-diffusive processes. Both subdiffusive and superdiffusive processes are typical of chaotic regimes. There are other types of transport identified by values of $\alpha = 2$ (ballistic motions i.e. at constant speed) and $\alpha = 3$ (for the separation of two random walker in turbulent motions). For the anomalous diffusion the probability distribution is not Gaussian (Klafter et al. 1987). The diffusion is often described by the diffusion equation, i.e. Fick's second law. This equation allows jumps with infinite speed, i.e. a jump with

an arbitrary length has a probability greater than zero. In contrast, the so called *telegraph model*, provides only the presence of finite speeds (Shlesinger et al. 1989). The diffusion equation applied to the probability density (with constant diffusion D = 1) is

$$\frac{\partial}{\partial t}\rho(\vec{r},t) = \frac{\partial^2}{\partial \vec{r}^2}\rho(\vec{r},t) \tag{3.3}$$

This diffusion equation has a Gaussian probability distribution and a linear dependence of standard deviation - time (Klafter et al. 1987). For the anomalous diffusion the form of the diffusion equation changes into

$$\frac{\partial}{\partial t}\rho(\vec{r},t) = \frac{\partial}{\partial \vec{r}}k(\vec{r},t)\frac{\partial}{\partial \vec{r}}\rho(\vec{r},t) \tag{3.4}$$

Passing to the space of Fourier-Laplace (i.e. doing a Fourier transform for the spatial component and a Laplace transform for the time component), the solution of the equation is

$$\rho(\vec{k},u) \sim \frac{1}{u} - C\frac{k^2}{u^{\alpha+1}} \tag{3.5}$$

3.1.2 Lévy flights versus Lévy Walks

The work of Lévy of the 20s and 30s led to the determination of non-Gaussian distributions with characteristics of scale invariance. In particular, Paul Lévy discovered the scale invariance when $p_n(k) = e^{-Cn|k|^b}$ ($p_n(k)$ is the Fourier transform of the probability distribution) with $b \in [0,2]$ and n which indicates the number of steps. b reveals the size of the set of points which is visited by Lévy Flight, and also identifies the type of distribution and therefore the type of movement: $b = 2$ we have Gaussian distribution then normal spread, $0 < b < 2$ indicates non-Gaussian distribution and anomalous diffusion, i.e. Lévy Flights.

As we can see from image (Fig. 3.1), the characteristic of the Lévy Flight is given by the presence of many short steps "connected" by a few long jumps. In this scheme, moreover, the displacements are considered immediate, which means to hypothesize infinite speed values. They follow a probability distribution:
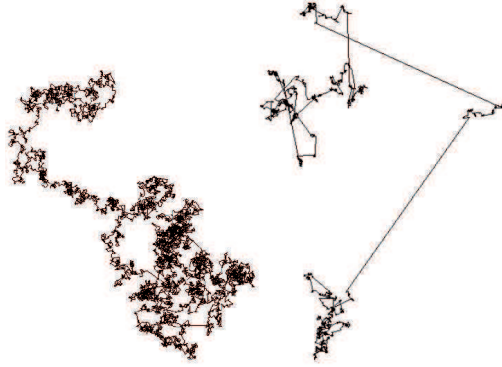
Figure 3.1 Random walk on the left *vs* Lévy flights on the right

$$p(\vec{r}) \sim |r|^{-\gamma-1} \tag{3.6}$$

The exponent γ is known as the Lévy index and varies between 0 and 2. A description of the characteristics of Levy Flights can be made by calculating the moments in different orders by using a probability distribution (PDF):

$$\langle x^n \rangle = \int_{-\infty}^{\infty} dx x^n P(x) \tag{3.7}$$

Assuming a decay in power law, that is, $P(x) \sim t^{-\mu}$, then for $n = 2$ and $\mu < 3$, the second moment diverges, and for $\mu \in]1,2]$ both the first and the second moment diverge, then the average length is infinite. With $\mu \in]2,3]$ the motion is intermediate between ballistic and normal. Taking "instant" steps (i.e. zero time), on one hand it reduces the applicability in the description of physical processes, on the other hand it highlights the impossibility of their "representation" in the Euclidean space. Starting from these considerations, we passed to the formalization of Lévy Walks for which, in fact, the time required to make a jump is not independent of the jump length.

In this context, the attention is placed on the distance traveled after a time *t* rather than on the entire shift. The distance traveled after a time *t* is called Lévy Walk. It remains to define a method for

making finished the standard deviation $\langle |r|^2 \rangle$ and in this case we can use the paradigm of CTRW (Continuous Time Random Walks) (Shlesinger et al. 1993) for which the motion can be characterized by "pauses" in certain positions by relaxing the constraint of the *instantaneous* passage from one point to another.

The CTRW approach is based on a probability distribution with the following form to describe the probability distribution to make a displacement *s* in time *t*

$$\Psi(\vec{r},t) = p(\vec{r})\delta(t - \frac{|\vec{r}|}{v}) \tag{3.8}$$

$v\vec{r}$ represents the length-dependent speed. The first factor, $p(\vec{r})$, is the probability of a trajectory, between two points at a distance $\vec{r}$. The term $\delta(t - \frac{|\vec{r}|}{v})$ can be interpreted as the conditional probability in the sense that, given the displacement $\vec{r}$, the time for that movement will be *t* (Shlesinger et al. 1993).

Another slightly different distribution which describes the Lévy Walks is

$$\Psi(\vec{r},t) = A(|\vec{r}|^{-\mu})\delta(|\vec{r}| - t^{\nu}) \tag{3.9}$$

where the delta function couples t and $\vec{r}$, any length jump is possible, but due to the coupling between t and $\vec{r}$, longer lengths are less likely. Lévy Walks are invariant in scale: the value of α in $\langle |\vec{r}|^2(t) \rangle \sim t^{\alpha}$ assumes different values depending on μ and the following relation $\alpha = 4 - \mu$ can be also applied.

In order to tie the statistics represented by the Lévy walks and the diffusion equation, i.e. the *physical* description of different types of transport, we can describe the relationship between the standard deviation of the trajectories and the diffusion coefficient. In the one-dimensional case the following relationship holds between the variance and the diffusion coefficient

$$\langle x^2(t) \rangle - \langle x(t) \rangle^2 = 2D't \tag{3.10}$$

Where D' is the diffusion coefficient and the term $\langle x^2(t) \rangle - \langle x(t) \rangle^2$ represents the variance $\sigma^2(t)$. It's clear that in the case of symmetric trajectories $\langle x(t) \rangle = 0$, the diffusion coefficient is directly

proportional to the standard deviation. Turning to the three-dimensional case, the variance can be defined as:

$$\langle x^2(t) \rangle + \langle y^2(t) \rangle + \langle z^2(t) \rangle = 6D't \tag{3.11}$$

and using the vector notation we can write:

$$\langle |\vec{r}|^2 \rangle = 2dD't \tag{3.12}$$

where d is the number of dimensions.

We define a diffusion coefficient D independent of time

$$D = \frac{\langle |\vec{r}|^2 \rangle}{t} \tag{3.13}$$

It is interesting to compare the time-independent diffusion coefficients obtained through the analysis of the standard deviation, with the coefficients obtained from the equation of Stokes-Einstein:

$$D' = \frac{k_B T}{6\pi \ni R} \tag{3.14}$$

Where k_B is the Boltzmann constant $\ni$ is the viscosity and R is the hydrodynamic radius: the higher viscosity and / or radius, the lower is the rate of diffusion. On the other hand, if the thermal energy increases ($\sim k_B T$), the spread is increased. The diffusion coefficients can be assumed to be time-dependent ((Weeks and Swinney 1998)), and be represented as follow:

$$D(t) = \Gamma t^{\alpha-1} \tag{3.15}$$

However, this type of dependency is problematic, since D diverges when t tends to 0 [sub-diffusion]. In any case, using this expression, we have

$$\langle |\vec{r}^2|(t) \rangle = D(t)t = \Gamma t^{\alpha} \tag{3.16}$$

For a Lévy Fligth, i.e. $\langle |\vec{r}^2|(t) \rangle = \infty$, the diffusion coefficient is infinite. It is noteworthy that, in the limit of Brownian motion, i.e. $\alpha = 1$, both the independent and dependent diffusion coefficients coincide $D(t) = constant = D$ so that $\langle |\vec{r}^2|(t) \rangle = Dt$. This means that the more the diffusion

coefficient $D(t)$ and D are different the more we move away from Brownian motion. Finally, fundamental to our work we report the relationship between the diffusion coefficient and a probability distribution using the following equation (one-dimensional case)

$$P(x,t) = \frac{1}{\sqrt{4\pi Dt}} e^{-x^2/4Dt} \tag{3.17}$$

Chapter 4

Direct simulation of Lévy Random Walk

In this chapter we describe the details of the numerical model proposed based based on Lévy Random Walk, giving a detailed description of both the used methodology and its implementation.

A large number of physical systems exhibits nondiffusive transport, that is, the mean square displacement of the random walker growing nonlinearly in time, $\langle \Delta x^2 \rangle \propto t^\alpha$ with $\alpha \neq 1$ (Bouchaud and Georges 1990; Metzler and Klafter 2000; 2004). In particular, when $\alpha > 1$ we have superdiffusion, and when $\alpha < 1$ we have subdiffusion. Such nonlinear growth is related to the presence of non Markovian, long memory properties in time, and/or to nonlocal, long range correlation properties in space (del-Castillo-Negrete et al. 2004; Perrone et al. 2013; Zaslavsky 2002). The long range correlation and long memory are frequently found to be associated with nonlinear maps (Geisel et al. 1985; Metzler and Klafter 2000), turbulent transport (Consolini et al. 2005; Klafter et al. 1987; Shlesinger et al. 1987; Zimbardo et al. 2000a; Zimbardo 2005; Zimbardo et al. 2010; **?**), and energetic particle transport in collisionless plasmas (Pommois et al. 2007; Shalchi and Kourakis 2007; Tautz 2010; Zimbardo et al. 2006). In particular, space plasmas, evidence of superdiffusion of energetic particles accelerated at interplanetary shocks was found by Effenberger (2012); Perri and Zimbardo (2007; 2008a; 2009a;b); Sugiyama and Shiota (2011), and evidence of superdiffusion of solar flare energetic particles by Trotta and Zimbardo (2011).

As proposed in the precious chapter, the superdiffusive transport can be described in terms of a Lévy random walk, that is in terms of a probabilistic description where the probability Ψ of a random walker making a free path of length x (forward or backward) in a time t is given by (Geisel et al. 1985; Klafter et al. 1987; Shlesinger et al. 1987)

$$\Psi(x,t) = A\,|x|^{-\mu}\,\delta(|x| - vt), \qquad |x| > x_0 \tag{4.1}$$

where $v > 0$ is the speed of the particle. In the Lévy walk description, it is essential to have a coupling between free path length and free path duration, as expressed by the delta function, in order to ensure the constant velocity of the particle undergoing the Lévy walk, as well as the conservation of energy. When such coupling is not present, a statistical process called Lévy flights is obtained (e.g., Consolini et al. 2005; Metzler and Klafter 2004), but this is not appropriate to describe the motion of single particles having mass, although it may be appropriate to other stochastic systems. In the above expression, it should be understood that the power-law form only applies for $|x| > x_0$, with x_0 a scale parameter, and that Ψ has a bell shaped profile for small x. It is important that for small values of the exponent μ "heavy", power law tails of Ψ are obtained, which correspond to a non negligible probability of very long free paths, corresponding to long range correlation. It is such non negligible probability which discriminates between a Lévy random walk leading to superdiffusion and a Gaussian random walk leading for normal diffusion.

It is readily verified that for $\mu < 3$ the mean square value of x, and hence the mean free path, is diverging,

$$\langle x^2 \rangle = \int x^2\,\Psi(x,t)\,dxdt \to \infty \qquad \mu < 3 \tag{4.2}$$

which means that the central limit theorem, does not require normal diffusion in this case (e.g., Bouchaud and Georges 1990; Klafter et al. 1987). Therefore, the free path probability distribution in Eq. (1) opens the gate to anomalous transport for $\mu < 3$. It can be shown that when $2 < \mu < 3$ the above free path probability leads to superdiffusion with (Geisel et al. 1985; Klafter et al. 1987;

Zimbardo et al. 2012; Zumofen and Klafter 1993)

$$\alpha = 4 - \mu. \tag{4.3}$$

Here it is seen that the power-law exponent μ has a primary role in determining the pace of su-
perdiffusion. It can also be shown that for $\mu < 2$ ballistic propagation is obtained, while for $\mu > 3$
normal diffusion is obtained, even if the random walk is composed of power-law distributed free
path lengths (e.g., Zumofen and Klafter 1993). As a consequence of the fact that a Lévy random
walk is described by a heavy tailed free path probability $\Psi(x,t)$ with diverging second order mo-
ment, the probability density function of the random walker positions $P(x,t)$ —the propagator— is
not a Gaussian. To leading order in the asymptotic expansion, the propagator is given by a modified
Gaussian for small $|x|$ (Metzler and Klafter 2004; Zumofen and Klafter 1993):

$$P(x,t) = \frac{A_0}{t^{1/(\mu-1)}} \exp\left(-\frac{x^2}{k_\mu t^{2/(\mu-1)}}\right) \tag{4.4}$$

and by a power-law for large $|x|$:

$$P(x,t) = A_1 \frac{t}{x^\mu} \qquad |x| < vt \tag{4.5}$$

with the propagator being zero for $|x| > vt$ because pf the δ-function coupling in Eq.(4.1). In
many cases it is desirable to carry out numerical simulation of the Lévy walk process, to com-
pare the simulation result with experimental data. In order to realize Monte Carlo simulations
of superdiffusion it is necessary to have a reliable implementation of the Lévy random walk,
as described in Eq. (4.1). Such a numerical implementation is useful for instance when the
source of superdiffusing particles is not point like, as assumed by Trotta and Zimbardo (2011),
or when propagation happens in a nonhomogeneous medium, so that the parameters μ and x_0
could vary with space and time. For instance, energetic particles propagation in the solar wind
can be described by constant μ and x_0 under the assumption of stationary turbulence properties,
(Perri and Zimbardo 2012a; Trotta and Zimbardo 2011), but data analysis shows that this is not

always the case(Perri and Balogh 2010a;b).

Here we present such a direct numerical simulation of a Lévy random walk in the 1-D case, and show that the theoretical predictions for the anomalous diffusion exponent $\alpha = 4 - \mu$ and the propagator, Eqs. (4.3,4.4) above, are well reproduced by numerical model (e.g., Effenberger 2012). We point out that while numerical implementations of Lévy flights are well known, see, e.g., Ghaemi et al. (2009), this is not the case for Lévy random walk. Indeed, the characterizing space-time coupling of Lévy walks requires that, once a long free path is extracted from the probability distribution $\Psi(x,t)$, the displacement length of the free path cannot be "given" to the random walker position disregarding time: a very long free path requires a very long time, too, so that special care is needed in computing the mean square displacement $\langle \Delta x^2 \rangle(t)$ and the propagator at a given time.

4.1 Numerical Method

The probability of free paths for Lévy random walk, given above, specifies the power law form of the probability for large x, (i.e. for $|x| > x_0$), while most authors do not specify the form for $|x| < x_0$, as this is not affecting the asymptotic behavior of $\langle \Delta x^2 \rangle$ and so on. A bell shaped form could be assumed, but in order to point out the unimportance of this point, we choose a flat distribution for $|x| < x_0$. Therefore, the form of the probability distribution related to the particle transport is characterized by two different expressions in relation to the value of the characteristic distance x_0 which represents the scale parameter, and, ultimately, the normalization length:

$$\Psi(x,t) = \begin{cases} \frac{1}{2}C\delta(|x| - vt), & x < x_0 \\[2em] \frac{1}{2}C|\frac{x}{x_0}|^{-\mu}\delta(|x| - vt), & x > x_0 \end{cases} \tag{4.6}$$

Here, v is the velocity of the diffusing particles, which is kept constant. In order to determining the value of the constant C, we use the following normalization condition

$$\int_0^{+\infty} dt \int_{-\infty}^{+\infty} dx \Psi(x,t) = 1 \tag{4.7}$$

Substituting (4.6) in (4.7), integrating in x, using the properties of $\delta(|x| - vt)$, using the symmetry of the distribution function, and separating the integration intervals in time using the relation $t_0 = x_0/v$ (also implied by the δ coupling), we obtain

$$\left[\int_0^{t_0} C dt + \int_{t_0}^{+\infty} C \left(\frac{vt}{x_0} \right)^{-\mu} dt \right] = 1 \tag{4.8}$$

We know that the superdiffusive transport is characterized by values of μ between 2 and 3 (e.g., Zumofen and Klafter 1993) so that $\lim_{t \to +\infty} \left[C \left(\frac{v}{x_0} \right)^{-\mu} \frac{t^{-\mu+1}}{1-\mu} \right] = 0$, that is, the above integral is converging. Ultimately, the value of the constant C can be obtained using the expression $C t_0 + C \left(\frac{v}{x_0} \right)^{-\mu} \frac{t_0^{1-\mu}}{\mu-1} = 1$, which also shows that for $\mu < 1$, $\Psi(x,t)$ cannot be normalized, and the condition $t_0 = x_0/v$:

$$C = \frac{1}{t_0} \left(\frac{\mu - 1}{\mu} \right) \tag{4.9}$$

We note that if a different profile of $\Psi(x,t)$ had been used for $|x| < x_0$, for instance a bell shaped function, this would simply change the value of $C t_0$ (i.e. the first contribution to the integral in Eq. (4.8)) into another constant. Now, we use the value obtained for C to determine the algorithm that allows to generate random numbers corresponding to the properties of distribution function (4.6). In other words, we want to find a relationship between a random number generated using a constant probability, and a number belonging to our probability distribution function (4.6). Let ξ be a random number evenly distributed in the range [0,1]. Sequences of random numbers ξ are generated by standard routines. The normalization conditions associated with two different

distributions (i.e., the constant distribution and the Lévy distribution), yields the following equation (e.g., Greco et al. 2002)

$$\psi(t)dt \equiv \left[\int_{-\infty}^{\infty} dx \Psi(x,t) \right] dt = C_\xi d\xi \tag{4.10}$$

where we used the fact that because of the δ coupling we can express ψ as a function of time only. Since ξ is distributed between 0 and 1 with constant probability, the normalization constant $C_\xi = 1$. Then we obtain an expression that relates ξ with t

$$\xi = \int_0^t \psi(t') \, dt' = \begin{cases} Ct & t < t_0 \\ \\ Ct_0 + C \int_{t_0}^t \left(\frac{vt'}{x_0} \right)^{-\mu} dt' & t > t_0 \end{cases} \tag{4.11}$$

Solving the integral in (4.11) $\int_{t_0}^t \left(\frac{vt'}{x_0} \right)^{-\mu} dt'$, and substituting (4.10) in (4.11), we obtain

$$\xi = \int_0^t \psi(t') \, dt' = \begin{cases} Ct, & \xi < \xi_0 \\ \\ Ct_0 + C \left(\frac{v}{x_0} \right)^{-\mu} \frac{1}{\mu-1} \left[t_0^{1-\mu} - t^{1-\mu} \right], & \xi > \xi_0 \end{cases} \tag{4.12}$$

where we have used the expression $\xi_0 = \frac{\mu-1}{\mu}$. To obtain the value of t as a function of ξ, we must reverse the expression (4.12), using the value of C (i.e. (4.9)) obtained from normalization condition of the distribution function. After some algebra we obtain the following expression for $\xi > \xi_0$

$$t = t_0 \left[\frac{1}{\mu(1-\xi)} \right]^{\frac{1}{\mu-1}} \tag{4.13}$$

while, clearly, $t = \xi/C$ for $\xi < \xi_0$.

Because of the specific space-time coupling of Lévy walks, a very long jump requires a very long time. On the other hand, when constructing a random walker trajectory by a Monte Carlo

methods, one usually gives a random displacement Δx_n at each regular interval Δt, where Δt represents the "granularity" of time intervals. In the present case, a long jump is to be divided in segments of length Δx_{ni}, such that $\Delta x_{ni} = v\Delta t$, with $\Delta t_n = k \times \Delta t$, with Δt_n being generated by the above procedure, Eqs. $(4.12 - 4.13)$, and the integer k running from 1 to $\Delta t_n / \Delta t$. In this way the set of position and times $(\Delta x_n, \Delta t_n)$ is used to construct the trajectory visited by Lévy walker. Denoting the current position and current time by uppercase X_n and T_n, we can represent the trajectories as

$$
\begin{cases}
X_n = x_0 + \sum_n \Delta x_n \\
\\
T_n = t_0 + \sum_n \Delta t_n
\end{cases}
\tag{4.14}
$$

where $\Delta x_n = \pm v\Delta t_n$, and for long jumps (i.e $\Delta t_n > \Delta t$)

$$
\begin{cases}
\Delta x_n = \pm \sum_i \Delta x_{ni} \\
\\
\Delta t_n = \sum_i \Delta t_{ni}
\end{cases}
\tag{4.15}
$$

The method used for the construction of the distribution function associated to the trajectories of the particles belonging to a simulation run, starts by determining the position of trajectories at a given time. In particular, once defined the granularity of the spatial intervals, a histogram is built for the determination of the number of particles belonging to a certain range (distribution function). The algorithm used to determine the distribution function, uses a linear interpolation that allows to reconstruct all the points of the trajectory, at each given intermediate time $t_i = i \times \Delta t$ based on the size of the intervals used for the histograms, so as to assign the correct number of particles at each time and each spatial interval defined. This procedure is particularly relevant for the long jumps of the particles, for which it is necessary to calculate the intervals crossed and the crossing time to build the distribution function using the information relating to all the trajectories. Ultimately, for each jump, we determine the number of intervals crossed by the walk and, using linear interpolation, thus determining the entire path from the starting point of the jump to the point

of arrival.

4.2   Simulation results

The numerical results are shown in figures 4.1 - 4.6 for different values of the Lévy power law index μ. We considered different values of $2 < \mu < 3$ to study superdiffusion, and values of $\mu > 3$ to study how normal diffusion is recovered. For each value of μ, we present the mean square displacement $\langle \Delta x^2 \rangle$ as a function of time, and the probability density function $P(x,t)$ of the random walker position at a different times; the latter is shown both in log-lin axes and log-log axes. Usually, 10^6 trajectories have been integrated for each run, while the integration time has been varied in order to reach the "asymptotic regime" in each case. Figure 4.1 show the simulation results for $\mu = 2.1$. The fit of $\langle \Delta x^2 \rangle \propto t^\alpha$ shows that $\alpha \cong 1.851$, in good agreement with the predicted value $\alpha = 4 - \mu = 1.9$. The propagator shows power law tails for large x, and a rounded peak for small x, as expected, with a smooth transition from the form of Eq.(4.4) to that of Eq. (4.5). The cutoff of the propagator for $|x| > vt$ is also visible from the middle panel in Figure 4.1, as the power law tail appear to go to zero at about $x = 3 \times 10^3 x_0$. Further, for all of Figures 4.1 - 4.4 it can be seen that the propagator decreases in time for small $|x|$, in agreement with Eq.(4.4) and increase in time for large $|x|$ in agreement with Eq.(4.5). This same behaviour of propagator is found in Figures $4.2, 4.3, 4.4$ for $\mu = 2.3, 2.7, 2.9$, respectively.

Figure 4.2 show the simulation results for $\mu = 2.3$, and it can be seen that $\alpha \cong 1.694$, in good agreement with the predicted value $\alpha = 4 - \mu = 1.7$.

Similar result are shown in Figure 4.3 and 4.4, all showing that the relation $\alpha = 4 - \mu$ is well verified (see also Table 4.1). We point out that this relation is a distinctive property of Lévy random walks, (e.g., Klafter et al. 1987; Zumofen and Klafter 1993), whereas superdiffusion described by fractional derivative on space yields $\alpha = \frac{2}{(\mu-1)}$ (e.g., Perrone et al. 2013; Zimbardo 2005). There-

fore we can say that our numerical model appropriately describes the Lévy random walk. On the other hand, the value of abscissa of the middle panel of Figures 4.1 - 4.4 for which $P(x,t)$ is appreciably different from zero, decreases with the increase of μ. In other words, the propagator is progressively less wide when μ increases. Clearly, this corresponds to the fact that the power law tail of the probability $\Psi(x,t)$ become less important, and the pace of transport is reduced, as is also shown by the values of $\langle \Delta x^2 \rangle$ for different μ.

The bottom panel of the figures shows the propagator in log-log axes, in order to appreciate the presence of the power-law tails. For Figures $4.1 - 4.4$ we have represented the "theoretical" slope, $P(x) \sim |x|^{-\mu}$, by dashed lines (on both sides of the numerical results). We can see that the theoretical slope of the tails is rather well reproduced by the numerical simulation in Figures 4.1 and 4.2. Conversely, the tails of the propagator for $\mu = 2.7$ and 2.9, reported in Figures 4.3 and 4.4, respectively, are somewhat steeper than the theoretical slope. We consider that this is not a shortcoming of the numerical model, but rather the manifestation of the fact that the propagator expressions given in Eq.$(4.5 - 4.4)$represent the leading term of the expansion for the Fourier-Laplace transform propagator for Lévy walk, see (Zumofen and Klafter 1993). If the expansion is carried out to higher order terms, additional, more steep asymptotics for the propagator are obtained, see (del-Castillo-Negrete et al. 2004). Indeed, such steeper-than-leading-term-propagator tails are also obtained by Blumen et al. (1990) by a numerical inversion of the Fourier-Laplace transform of the propagator, as given by the Montrell-Weiss equation.

Figure 4.5 shows the result for $\mu = 3.2$, that is for a value of μ larger then 3, for which normal diffusion is expected. Indeed, Figure 4.5 shows that mean square deviation grows as t^α with $\alpha = 1.01$, that is, normal diffusion in practice. Also the shape of $P(x,t)$ is rather similar to a Gaussian although a small power law tail can be seen for large $|x|$. As shown by Zumofen and Klafter (1993) this power-law tail of the propagator is to be expected for $3 < \mu < 4$, even though the pace of transport is diffusive.

Finally, Figure 4.6 shows the result for $\mu = 4.5$, that is for a value of μ which corresponds to normal diffusion and a Gaussian distribution function (e.g., Zumofen and Klafter 1993): both prediction are confirmed, with $\alpha = 1.0092$ and a clearly Gaussian $P(x,t)$. As expected, the values of $\langle \Delta x^2 \rangle$ and the width of $P(x,t)$ are much less than in the previous cases, due to the scarcity of long jumps. The simulation results, including a few more cases which are not shown, are summarized in Table 4.1.

μ	α_{sim}	α_{theory}
2.1	1.850	1.9
2.3	1.694	1.7
2.5	1.528	1.5
2.7	1.247	1.3
2.9	1.067	1.1
3.2	1.014	1.0
3.5	1.012	1.0
4.5	1.009	1.0

Table 4.1 Numerical simulation results. The column μ is the exponent that determines the pace of superdiffusion (i.e. $\alpha = 4 - \mu$). The column α_{sim} is the value computed by numerical simulation. The column α_{theory} is the value predicted from the theory.
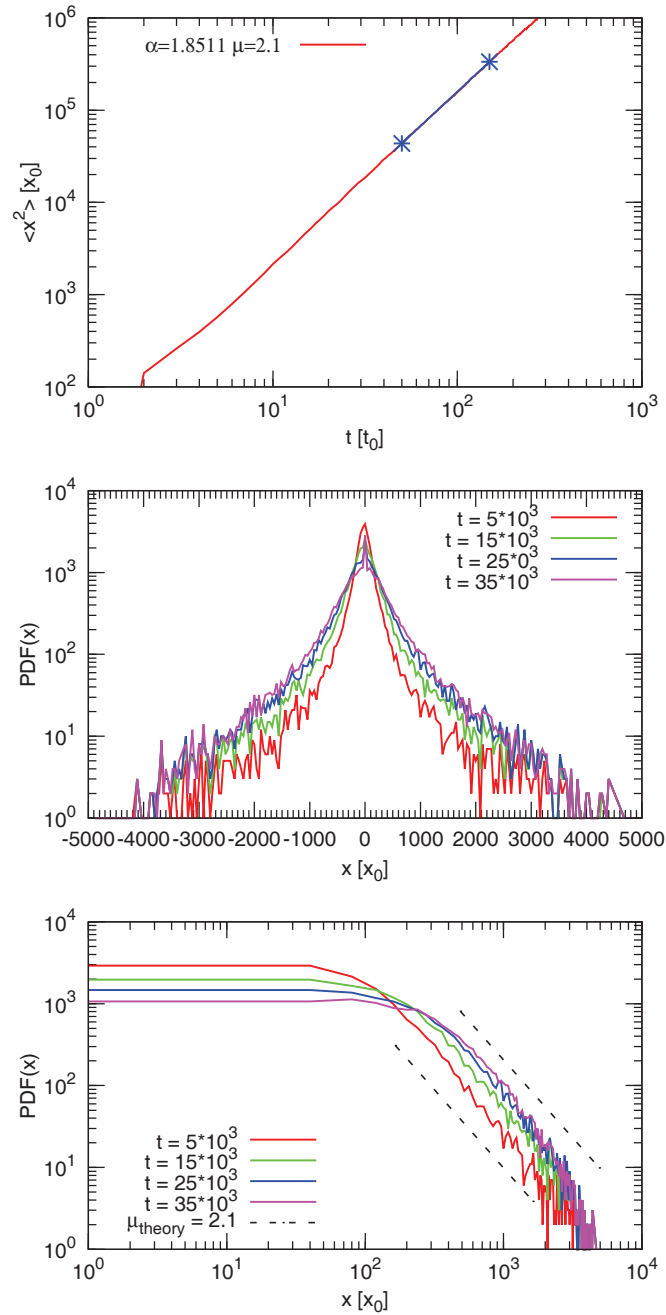
Figure 4.1 Numerical results for $\mu = 2.1$. Top panel: fit of the mean square displacement versus time. Middle panel: the probability distribution function (PDF) of positions for different times in log-lin axes. Bottom panel: the same PDF for $x > 0$ in log-log axes. The dashed lines represent the theoretical slope μ.
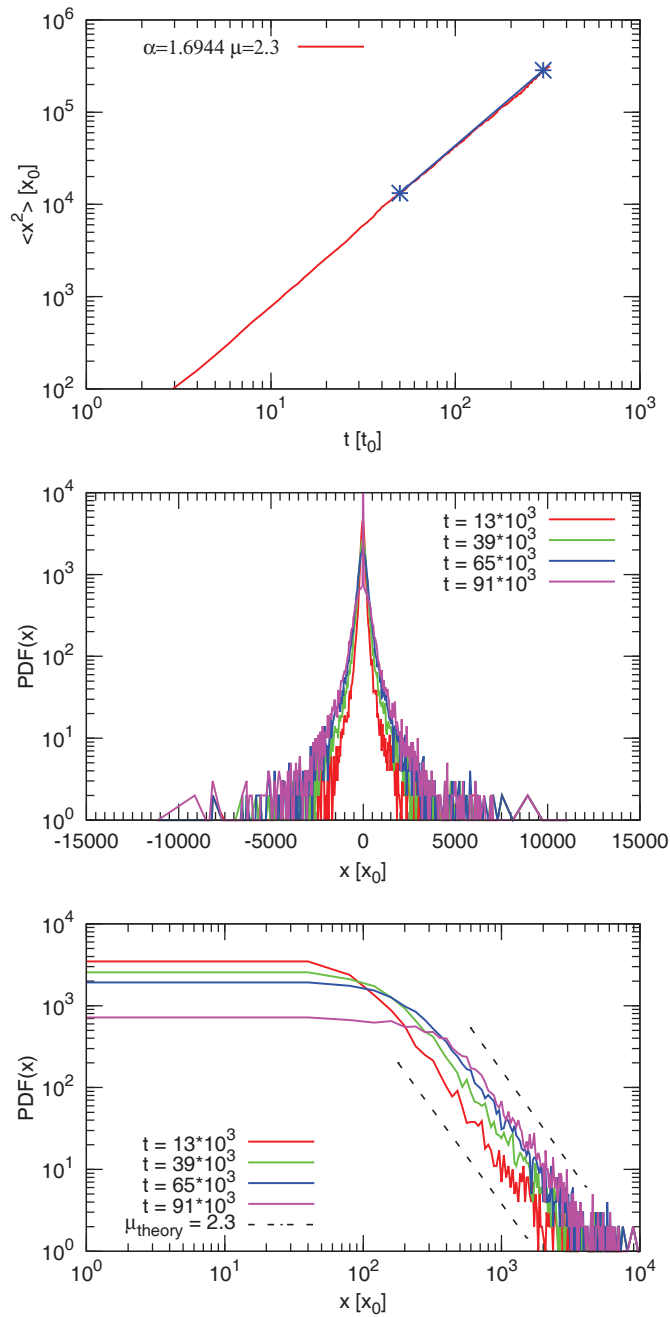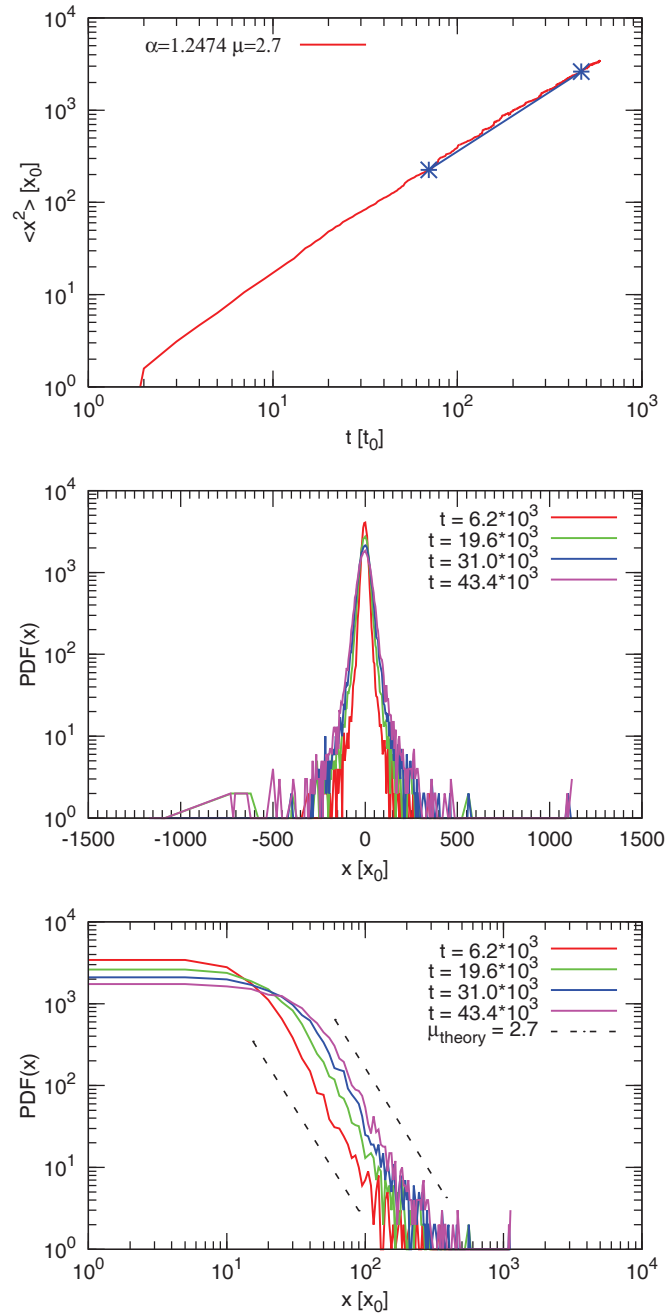
Figure 4.2 Numerical results for $\mu = 2.3$. Top panel: fit of the mean square displacement versus time. Middle panel: the probability distribution function (PDF) of positions for different times in log-lin axes. Bottom panel: the same PDF for $x > 0$ in log-log axes. The dashed lines represent the theoretical slope μ.
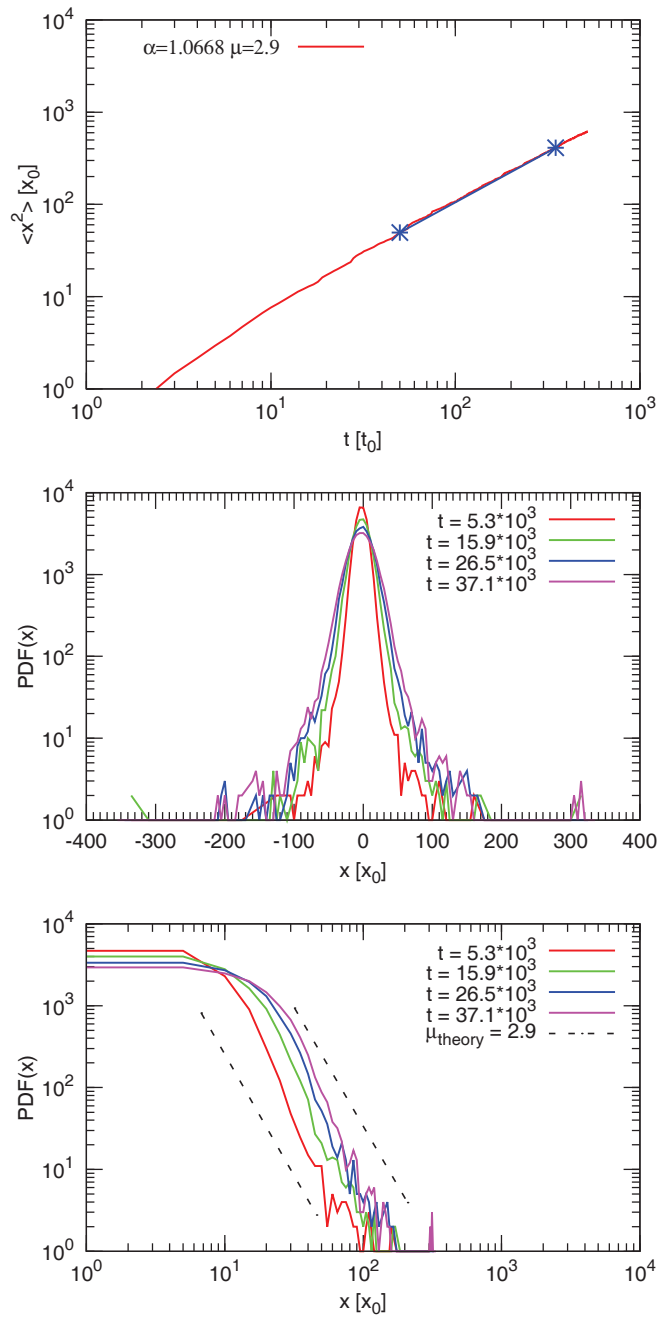
Figure 4.3 Numerical results for $\mu = 2.7$. Top panel: fit of the mean square displacement versus time. Middle panel: the probability distribution function (PDF) of positions for different times in log-lin axes. Bottom panel: the same PDF for $x > 0$ in log-log axes. The dashed lines represent the theoretical slope μ.
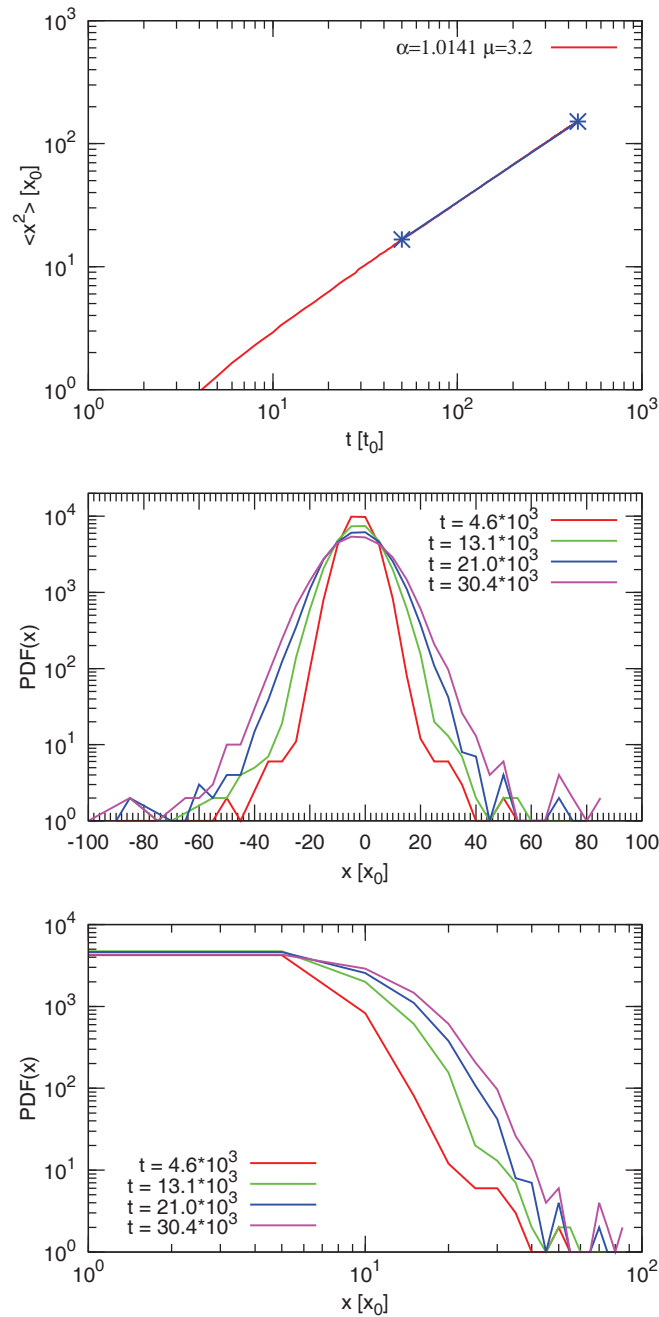
Figure 4.4 Numerical results for $\mu = 2.9$. Top panel: fit of the mean square displacement versus time. Middle panel: the probability distribution function (PDF) of positions for different times in log-lin axes. Bottom panel: the same PDF for $x > 0$ in log-log axes. The dashed lines represent the theoretical slope μ.

Figure 4.5 Numerical results for $\mu = 3.2$. Top panel: fit of the mean square displacement versus time. Middle panel: the probability distribution function (PDF) of positions for different times in log-lin axes. Bottom panel: the same PDF for $x > 0$ in log-log axes.
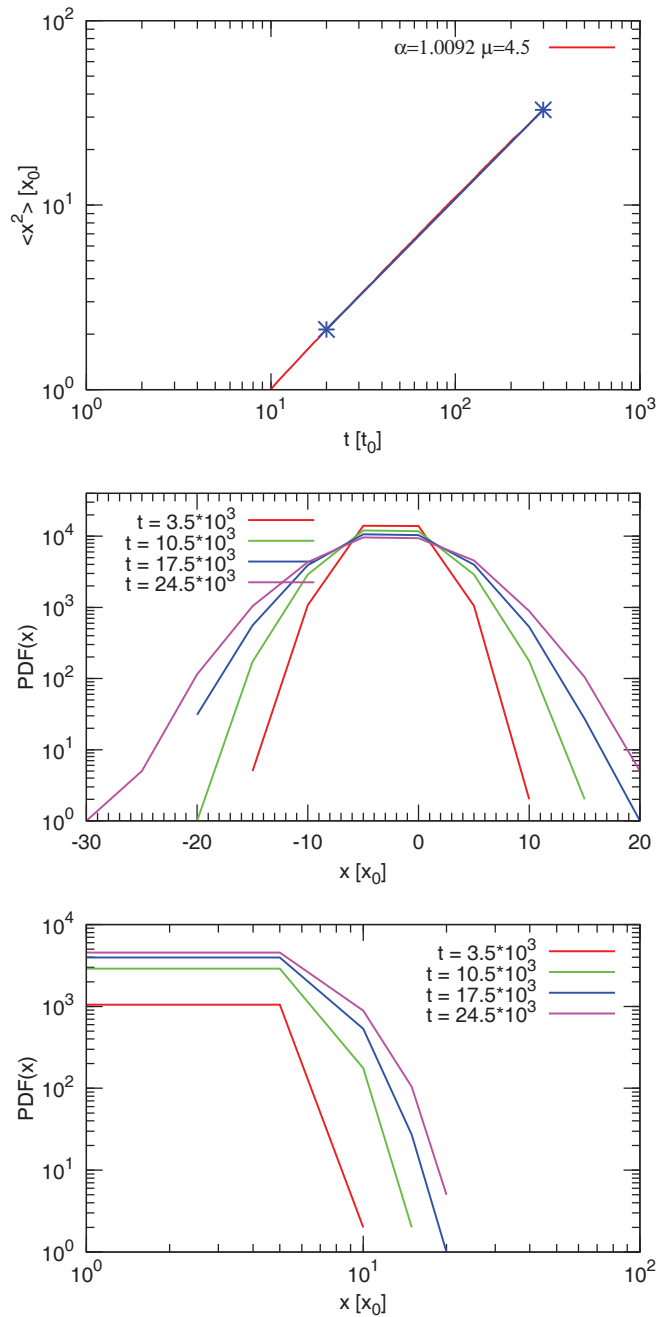
Figure 4.6 Numerical results for $\mu = 4.5$. Top panel: fit of the mean square displacement versus time. Middle panel: the probability distribution function (PDF) of positions for different times in log-lin axes. Bottom panel: the same PDF for $x > 0$ in log-log axes.

Chapter 5

Test particle simulation for impulsive events

In this chapter we will give the details of the test particle simulation for steady of motion of energetic particles in solar wind. Also, with the help of the various figures, we will show the results obtained with the different runs performed in the simulation. The chapter starts with the description of the main characteristics of the equation used in numerical simulation (i.e.*the drift approximation*). Then a brief description of the numerical programs is given. Subsequently, are illustrated the various runs performed by adding to the first term of the equation of motion of the guiding center, the various terms of drift due to electric and magnetic fields crossed at the gradient of the magnetic field and the curvature of the lines of force, and different diffusion models . Finally, we will show some examples of comparison between numerical results and observed data .

As we said in previous chapter, in recent years, the study of transport phenomena linked to phenomena such as CME and flare has been much developed. In particular, the study focused on the analysis of the temporal profiles of the flows of electrons and ions associated with these events (Cane et al, 1988;. Reames, 1999). The particles involved in this kind of phenomena (ions that can reach energies up to 1 GeV), can reach distances that exceed 1 AU with a motion strongly linked to the shock caused by the CME. The SEP phenomena of long duration (several days) are classified as gradual events. The gradual events observed are often associated with the CME that,

also by virtue of the interaction with the interplanetary magnetic field, it expands moving outward. The interaction of the particles with the shock produced by the CME determines the characteristics of the transport itself. There are several theoretical works related to the study of the motion of these particles and their transport characteristics (Lee, 1983, 2005; Reames and Ng, 1994; Giacalone and Kota 2006) using the paradigma based on the diffusive motion and the dispersion of the waves, which involve the solution of the Boltzmann equation in spherical geometry for finding both analytical and numerical solutions for the transport analysis of gradual events. In particular, these studies deal with the motion of particles through a magnetic field given with fluctuations linked to phenomena of turbulence with a certain degree of correlation. The construction of "realistic" models for gradual SEP events are a challenge for simulations of space weather because of their fundamental importance in predicting risk intrinsically linked to events of this kind. There are several numerical models for the study of shock and consequent phenomena of particle acceleration aimed at the study of the temporal profiles associated with SEP. All these models use different types of simplifying assumptions in order to make the problem tractable from the mathematical and / or computational point of view. In general, the problem of modeling a gradual event shows strong difficulty (currently unresolved) in the relationship between the properties of the impacts and aspects diffusive / super-diffusive of motion of the particles. A useful approach to the study of these phenomena could be based on the properties of Lévy random walk to be used for the study of transport characteristics in gradual events: set the template to use for the description of the shocks associated with CMEs, the properties of motion of the particles through the shock can be modeled using, in fact, the levy random walk.

5.1 Motion of particles in drift approximation

A plasma is an electrically neutral gas mainly composed of charged particles. The role of the electromagnetic field is essential to understand the behavior of the plasma. Although many phenomena related to plasma are of a collective nature, we can see, in this chapter, some aspects of the interaction between electromagnetic fields and the single particle. For a particle of mass m and charge q placed in an electromagnetic field B the non-relativistic equation of motion is

$$\frac{dv}{dt} = \frac{q}{m}(\vec{E} + \frac{\vec{v} \wedge \vec{B}}{c}) \tag{5.1}$$

This equation will be solved for some configurations and conditions of the electromagnetic field. As it is already known, in a uniform magnetic field the charged particles move along a helical paths, with the axis of the helix along the magnetic field. In the presence of electric and non-uniform fields the motion is more complicated. If the electric field and the non-uniformity are not too strong, the motion of the particles can be described as a circular motion (perpendicular to the magnetic field) superimposed on a motion of "drift" in the center of the orbit. We are talking about motion in the drift approximation, and this introduces the concept of guiding center.

In space plasma, despite the presence of an electric field, it is often possible to assume that the component of said electric field parallel to the magnetic field disappears (i.e. $\vec{E_0}.\vec{B_0} = E_0 B_0 = 0$). It is because 5.1 tells us that only the electric field can exert a force in the direction of B_0. This force moves the positively charged particles in the direction of E_0 and those negatively charged in the opposite direction. If there is a sufficient number of particles, their relative displacement can produce a field, due to the charge separation, which grows opposing E_0 until it is cancelled; after that no force will act in the direction of the magnetic field. The response of charged particles to the perpendicular component of E_0 is very different. To understand this motion let's think first about how the charges move the charges move when there is only B_0, they whirl in a circle, the direction of the motion depends on the sign of the charge and the radius of the circle, ρ, varies with the mass

of the particle. Hence, ρ is higher for a ion that for an electron, and, at a given speed, the electric field accelerates the particle along a part of the orbit, and decelerates along the remaining part, the result is that the orbit is a cycloid or trochoid with a radius of curvature wider for half orbit and narrower for the remaining half. To analyze the problem let's think as in the previous case, decomposing the equation of motion along the coordinate axes, in the simplificative assumption that E_0 and B_0 are "crossed", placing B_0 along the z axis and E_0 along the x axis. At this point 5.1 decomposes into

$$\left[\begin{array}{l} \ddot{x} - \frac{qB_0}{mc}\dot{y} = \frac{q}{m}E_{0\perp} \\ \ddot{y} - \frac{qB_0}{mc}\dot{x} = 0 \end{array} \right. \tag{5.2}$$

so we have

$$(\ddot{x} + i\ddot{y}) + i\frac{qB_0}{mc}(\dot{x} + i\dot{y}) = \frac{q}{m}E_{0\perp} \tag{5.3}$$

by introducing complex variable $\omega = \dot{x} + i\dot{y}$, we can write

$$(\dot{\omega} + i\Omega\omega) = \frac{q}{m}E_{0\perp} \tag{5.4}$$

the solution of the homogeneous equation associated with 5.4 is

$$\omega_0 = v_\perp e^{-i(\Omega t + \phi)} \tag{5.5}$$

For the particular solution we cab think as follows, such a solution is a constant so we put the total solution as $\omega = \omega_0 + A$ where A is a constant function. So we obtain

$$\dot{\omega} + \dot{A} + i\Omega(\omega + A) = \frac{q}{m}E_{0\perp} \tag{5.6}$$

using $\dot{\omega} + i\Omega\omega = 0$ and $\dot{A} = 0$ we obtain

$$A = -\frac{i}{\Omega}\frac{q}{m}E_{0\perp} \tag{5.7}$$

Factoring it in the real and imaginary parts, we obtain

$$\left[\begin{array}{l} v_x = v_\perp cos(\Omega t + \phi) \\ v_y = -v_\perp sin(\Omega t + \phi) - \frac{cE_{0\perp}}{B_0} \end{array} \right. \tag{5.8}$$

and integrating previous relations we reach the following result

$$
\begin{bmatrix}
x = x_0 + \frac{v_\perp}{\Omega} sin(\Omega t + \phi) \\
y = y_0 + \frac{v_\perp}{\Omega} cos(\Omega t + \phi) - \frac{cE_{0\perp}}{B_0} t
\end{bmatrix}
\tag{5.9}
$$

Now, we define the guiding center as the point that represents the center of the orbit and that moves, in this case, according to the law

$$
\begin{bmatrix}
x = x_0 \\
y = y_0 - \frac{cE_{0\perp}}{B_0} t
\end{bmatrix}
\tag{5.10}
$$

This means that the guiding center "drifts" in the direction perpendicular to B_0 and to E_0 with speed, called the drift velocity, equal to

$$
v_E = -\frac{cE_{0\perp}}{B_0} \hat{e}_y = \frac{\vec{E}_{0\perp} \wedge \vec{B}_0}{|\vec{B}^2|} c
\tag{5.11}
$$

We talk about motion in the drift approximation to indicate that the motion of the particle is done by the sum of the circular motion, in the Way dependent on the charge of the particle, added to the motion of the guiding center. The drift due to the fields E_0 and B_0 crossed does not introduce currents in the plasma, since v_E is independent of both q and m.

In the previous discussion, B was assumed to be uniform, it means that its intensity and its direction do not change for each point of the system. Although sometimes this might be a good approximation, very often it cannot be applied. For example, the Earth's magnetic field can be considered equivalent, in a first approximation, to a magnetic dipole that changes in direction and magnitude both longitudinally and transversely. Then, it is compulsory a description of the motion of a particle in a variable magnetic field. The field $\vec{B}$ gradient and, in the more general case, a tensor of nine components but, if the field varies along a single direction, it may be expressed only in function of the module $\vec{B}$, namely in the following way

$$
\nabla B = (\frac{\partial B}{\partial x}, \frac{\partial B}{\partial y}, \frac{\partial B}{\partial z})
\tag{5.12}
$$

A technique to study the motion that results from the terms of the gradient in a magnetic field, is to consider a series of simplified problems that take into account any type of term individually, and then to sum the effects and obtain the Total motion. The only simple cases are those in which the spatial variations of the field $\vec{B}$ are small, that is to say that the field does not change in distances comparable with the cyclotron radius ρ, i.e. $\rho/R << 1$ where R indicates the scale of variation of $\vec{B}$. Let calculate the different terms that influences the drift motion, starting with the case $\nabla b || \vec{B}$. Consider a charged particle that circles around the axis of symmetry of a $\vec{B}$ field with cylindrical symmetry. Suppose that $\vec{B}$ grow in function of the distance along the axis of symmetry. Writing the divergences in cylindrical coordinates, and integrating we get B_r, in terms of B_z. Assuming that the variation of B_z along z (i.e. $\frac{\partial B}{\partial z}$) is small, that is, assuming that the rate of convergence of the lines of force of $\vec{B}$ is constant, we can carry out of the integral that term obtaining

$$B_r = -(\frac{r}{2}\frac{\partial B}{\partial z}) \tag{5.13}$$

Note that if B_z grows with z, i.e. $\partial B/\partial z > 0$, the radial component of the magnetic field is negative, and is directed towards the z axis. Now, there is a component of the magnetic force, acting on the particle along the axis of the orbit, due to the component of B which determines the reflection of the particle, this phenomenon is called the *magnetic mirror*. This phenomenon can be expressed in terms of the energy of the particle and the magnetic field as follows

$$\mu = \frac{1}{2}\frac{mv_\perp^2}{B} \tag{5.14}$$

that can be generalized to give the force parallel to the magnetic field

$$\vec{F}_\parallel = -\vec{\mu}.\nabla B \tag{5.15}$$

Where $\vec{\mu} = \mu \hat{e}_B$ with $\hat{e}_B$ unit vector in the direction of $\vec{B}$ equal to $\hat{e}_B = \vec{b}/|\vec{B}|$ The quantity μ is also called *first adiabatic invariant*, where *adiabatic* refers to the condition that μ is invariant if the system parameters, such as the intensity and direction of the field, vary slowly. We can describe

the mechanism of the magnetic mirror using μ and the constant of motion W (= total energy of the system). In particular, the point at which occurs the phenomenon of magnetic reflection, called point of magnetic mirror, the speed $v_{\parallel}$ is canceled, and then reversed. Consider the point z_0 in which there is the highest intensity B_{max}, of field $\vec{B}$ B. We can write

$$\frac{1}{2}mv_{\parallel 0}^2 + \mu B_0 = \frac{1}{2}m[v_{\parallel}(z_0)]^2 + \mu B_{max} \tag{5.16}$$

so that the particle exceeds the point of magnetic mirror must be $1/2mv_{\parallel 0}^2 + \mu B_0 > \mu B_{max}$ from which follows

$$\frac{v_{\parallel 0}^2}{v_{\perp 0}^2} > \frac{B_{max}}{B_0} - 1 \tag{5.17}$$

From (5.17) it is deduced that the fact that the particle exceeds the point of magnetic mirror does not depend on the energy that it possesses but by the ratio $v_{\parallel 0}^2/v_{\perp 0}^2$, in particular from α angle, said *angle of pitch*, that the speed of the particle forms under the direction of $\vec{B}$. We have $\tan\alpha = v_{\parallel}/V_{\perp}$, so in terms of the pitch angle the condition (5.17) becomes

$$\alpha_0 < \sqrt{\frac{B_0}{B_{max} - B_0}} \tag{5.18}$$

Then, if the pitch angle of the particle is higher than α_0, it exceeds the magnetic mirror, otherwise it is reflected.

Consider a unidirectional magnetic field with a gradient of the module perpendicular to its direction, i.e.$\nabla B \perp \vec{B}$. In such a field the particle will drift perpendicularly both to $\vec{B}$ and to ∇B. This is easily understood by noting that, when the particle moves in a strong field, its cyclotron radius becomes smaller, and when, in the remaining portion of its orbit, moving in a weak field the radius becomes bigger. While the particle spins, the orbit is not closed with the result that the particle drifts. The drift due to this type of gradient can be obtained by expanding the range $\vec{B}$ in Taylor series with respect to the center of the orbit, for assumed that moves slowly in time with respect to the orbital motion. The general expression for the speed of drift produced by an arbitrary constant

force $\vec{F}$ is

$$\vec{v}_F = \frac{c^2}{q} \frac{\vec{F} \wedge \vec{B}}{|\vec{B}|^2} \tag{5.19}$$

In our case, $\vec{F}$ is the magnetic force that takes into account the fact that $\vec{B}$ varies, so it is stronger on one side and weaker on the other, hence it is always considered an average made on the assumption $\rho/R << 1$. In fact, if we assuming that ∇B is directed along x, then evaluating the average force along x and develop B_x in Taylor series, we obtain

$$\langle \vec{F} \rangle = \frac{1}{2} \frac{q}{c} \frac{v_\perp^2}{\Omega} \nabla B \tag{5.20}$$

Then in the case of $\nabla B \perp B$ the drift velocity of the particles is given by

$$\vec{v}_{\nabla B} = \frac{c}{q} \frac{\langle \vec{F} \rangle \wedge \vec{B}}{|\vec{B}|^2} = -\frac{1}{2} \frac{v_\perp^2}{\Omega} \frac{\nabla B \wedge B}{|\vec{B}|^2} \tag{5.21}$$

since $\Omega = qB/mc$ we can write

$$\vec{v}_{\nabla B} = \frac{1}{2} \frac{m v_\perp^2}{q} \frac{v \, \hat{e}_B \wedge \nabla B}{|\vec{B}|^2} = \frac{c\mu}{q} \frac{\hat{e}_B \wedge \nabla B}{|\vec{B}|^2} \tag{5.22}$$

It should be noted that the speed of drift depends on the sign of the charge and can generate currents in the plasma and charge separation.

Now consider a magnetic field with the curvature of the lines of force, such as, for example, a simple dipole magnetic field. This field has a gradient perpendicular to its direction that causes the drift motion previously described. In addition to that, if the particle has a velocity parallel to $\vec{B}$, it undergoes a centrifugal force, due to the curvature of the field, in the direction perpendicular to both the field $\vec{B}$ and the radius of curvature R_c. We define R_c as the vector radially directed and with module equal to the radius of curvature. The speed of drift due to this centrifugal force is expressed as

$$\vec{v}_{R_c} = \frac{1}{q} \frac{\vec{F}_c \wedge \vec{B}}{|\vec{B}|^2} \tag{5.23}$$

where the centrifugal force $\vec{F}_c = \hat{e}_{R_c} m v_\parallel^2 / |\vec{R}_c|$ therefore the speed of drift is

$$\vec{v}_{R_c} = \frac{mc}{q} |\frac{\vec{v}_\parallel}{\vec{R}_c}|^2 \frac{\vec{R}_c \wedge \vec{B}}{|\vec{B}|^2} \tag{5.24}$$

We have previously defined the guiding center as the point representing the center of the orbit of the particle, we have also seen that, in cases of crossed electric and magnetic fields, ∇B perpendicular to $\vec{B}$, magnetic field curvature, the guiding center undergoes a motion of drift compared to the original trajectory followed by the particle, for this reason, it is called motion in the drift approximation. The overall motion of the particle can be described by adding to the original motion the various present terms of drift. If the position vector $\vec{r}$ describes the trajectory of the particle, the velocity vector is defined by the known relationship $\vec{v} = \frac{d\vec{r}}{dt}$ then considering the effects due to the crossed electric and magnetic fields, ∇B perpendicular to $\vec{B}$ and magnetic field with curvature we can write the relation, which describes the motion of the particle considered in the drift approximation, as follows

$$\vec{v} = \frac{d\vec{r}}{dt} + \frac{\vec{E}_{0\perp} \wedge \vec{B}_0}{|\vec{B}_0|^2}c + \frac{\mu c}{q}\frac{\hat{e}_B \wedge \nabla B}{|\vec{B}|^2} + \frac{mc}{q}|\frac{\vec{v}_\parallel}{\vec{R}_c}|^2\frac{\vec{R}_c \wedge \vec{B}}{|\vec{B}|^2} \tag{5.25}$$

5.2 Numerical Simulation

The equations of motion in the drift approximation, which we will use after, are the following

$$\left[\begin{array}{l} \frac{d\vec{r}}{dt} = v_\parallel \frac{\vec{B}}{B} + \frac{\vec{E} \wedge \vec{B}}{B^2} + \frac{\mu}{q}\frac{\vec{B} \wedge \nabla B}{B^2} + \frac{mv_\parallel^2}{q}\frac{\vec{B} \wedge (\vec{B}.\vec{\nabla})\vec{B}}{B^4} \\ \frac{d\vec{v}_\parallel}{dt} = -\frac{\mu}{m}\nabla B.\frac{\vec{B}}{B} \end{array}\right. \tag{5.26}$$

where $\vec{r}$ is the position of the particle, m and q are the mass and the charge, $\vec{v}_\parallel$ is the component of the velocity of the particle parallel to the direction of the magnetic field, $\mu = \frac{mv_\perp^2}{2B}$ is the magnetic moment of the particle, $\vec{B}$ is the magnetic field in the solar wind according to the model of Parker. The various terms in the first of (5.26) correspond, respectively, as we have shown in the previous paragraph, to the motion of the guiding center along the magnetic field, to the drift motion caused by the presence of crossed electric and magnetic fields, by the gradient of the magnetic field and by the curvature of the lines of force of the field itself. In spherical coordinates the magnetic field

is written as

$$
\begin{cases}
B_r = B_{rE}\left(\frac{r_E}{r}\right)^2 \\[2mm]
B_\theta = 0 \\[2mm]
B_\phi = B_{rE}\left(\frac{r_E}{r}\right)^2 \frac{\Omega r}{V_{sw}} \sin(\theta)
\end{cases}
\tag{5.27}
$$

As regards the first of (5.26), in spherical coordinates it is decomposed in the following way

$$
\begin{cases}
\frac{dr}{dt} = v_\parallel \frac{B_r}{B} + V_{sw} \frac{B_\phi^2}{B^2} - \frac{\mu}{q} \frac{B_\phi \nabla_\theta B}{B^2} \\[2mm]
\frac{d\theta}{dt} = \frac{\mu}{qr} \frac{B_\phi \nabla_r B}{B^2} + \frac{mv_\parallel^2}{qr}\left(-\frac{B_r^2}{B^4}\frac{\partial B_\phi}{\partial r} + \frac{B_r B_\phi}{B^4}\frac{\partial B_r}{\partial r}\right) \\[2mm]
\frac{d\phi}{dt} = \frac{v_\parallel}{r sin\theta} \frac{B_\phi}{B} - \frac{V_{sw}}{r sin\theta} \frac{B_r B_\phi}{B} + \frac{\mu}{qr sin\theta} \frac{B_r \nabla_\theta B}{B^2}
\end{cases}
\tag{5.28}
$$

where ∇_r and ∇_ϕ are, respectively, the radial and the polar component of the gradient of the module of magnetic field, calculated in spherical geometry and B is the module of the magnetic field of Parker

$$
B = |\vec{B}| = B_{rE}\left(\frac{r_E}{r}\right)^2 \left[1 + \left(\frac{\Omega r}{V_{sw}}\right)^2 \sin^2\theta\right]^{1/2}
\tag{5.29}
$$

Substituting 5.29 in 5.28 and using $\nabla \vec{B} = \left(\frac{\partial B}{\partial r}, \frac{1}{r}\frac{\partial B}{\partial \theta}, \frac{1}{r sin\theta}\frac{\partial B}{\partial \phi}\right)$ after some algebra our system of equations became

$$
\begin{cases}
\frac{dr}{dt} = v_\parallel[1+a^2]^{-1/2} + V_{sw}a^2[1+a^2] + \frac{\mu}{qr}\frac{\Omega r}{V_{sw}}a^2\cos\theta[1+a^2]^{-3/2} \\[2mm]
\frac{d\theta}{dt} = \frac{\mu}{qr^2}a[1+a^2]^{-1/2}[2-a^2[1+a^2]^{-1}] + \frac{mv_\parallel^2}{qr}a[B_{rE}(\frac{r_E}{r})^2[1+a^2]^2]^{-1} \\[2mm]
\frac{d\phi}{dt} = -v_\parallel\frac{\Omega}{V_{sw}}[1+a^2]^{-1/2} + \Omega[1+a^2]^{-1} + \frac{\mu}{qr^2}(\frac{\Omega r}{V_{sw}})^2\cos\theta[1+a^2]^{-3/2} \\[2mm]
\frac{dv_\parallel}{dt} = \frac{\mu}{m}\frac{B_{rE}r_E^2}{r^3}[2-a^2[1+a^2]^{-1}]
\end{cases}
\tag{5.30}
$$

where $a = \left(\frac{\Omega r}{V_{sw}}\sin\theta\right)$ We can obtain the dimensionless equations by normalizing all lengths with the Scale of the simulation box L, that we place equal to the Earth-Sun distance, i.e. $L = r_E = 1.5 x 10^8 km$, the magnetic field with the average magnetic field to 1 AU, i.e. B_{rE}, the time with the cyclotron frequency in B_{rE}, $\omega_{rE} = qB_{rE}/m$, the speed with v_n, which we will specify later, and finally, the group $\mu B_{rE}/m$ with v_n^2. At this point, we define the new dimensionless variables

(indicated by a tilde sign) as follows

$$
\begin{cases}
\vec{\tilde{x}} = \frac{\vec{x}}{L} \\[4pt]
\vec{\tilde{B}} = \frac{\vec{B}}{B_{rE}} \\[4pt]
\tilde{t} = \frac{t}{\tau} = t\,\omega_{rE} = t\frac{qB_{rE}}{m} \\[4pt]
\vec{\tilde{v}} = \frac{\vec{v}}{v_n}
\end{cases}
\tag{5.31}
$$

then we can rewrite our equations in dimensionless form as

$$
\begin{cases}
\frac{d\tilde{r}}{d\tilde{t}} = v_e \tilde{v}_{\parallel}[1 + b\tilde{r}^2\sin^2\theta]^{-1/2} + v_e\frac{V_{sw}}{v_n}b\tilde{r}^2\sin^2\theta[1 + b\tilde{r}^2\sin^2\theta]^{-1} \\[4pt]
\frac{d\theta}{d\tilde{t}} = 0 \\[4pt]
\frac{d\phi}{d\tilde{t}} = -bv_e\tilde{v}_{\parallel}[1 + b\tilde{r}^2\sin^2\theta]^{-1/2} + \tau\Omega[1 + b\tilde{r}^2\sin^2\theta]^{-1} \\[4pt]
\frac{d\tilde{v}_{\parallel}}{d\tilde{t}} = \frac{v_e C}{\tilde{r}^3}\left[2 - b\tilde{r}^2\sin^2\theta[1 + b\tilde{r}^2\sin^2\theta]^{-1}\right]
\end{cases}
\tag{5.32}
$$

where

$$
\begin{aligned}
b &= \frac{\Omega L}{V_{sw}} \\[4pt]
C &= \frac{\mu B_{rE}}{mv_n^2} \\[4pt]
\tau &= \frac{mc}{qB_{rE}} \\[4pt]
v_n &= \sqrt{2E/m} \\[4pt]
v_e &= \frac{\tau v_n}{L}
\end{aligned}
\tag{5.33}
$$

Regarding the normalization constant C, it is calculated, in the program, once allocated the initial speed of the particle, in the following way

$$
C = \frac{\mu B_{rE}}{mv_n^2} = C = \frac{mv_{\perp}^2}{2B}\frac{B_{rE}}{mv_n^2} = \frac{1}{2}\frac{B_{rE}}{B}\tilde{v}_{\perp}^2
\tag{5.34}
$$

To evaluate the diffusion perpendicular (i.e. diffusion due to turbulence) to the average magnetic field, we integrate numerically (5.32) in a simulation box. The integration is made in a Cartesian system (fc, y, z), where the direction z is along the average magnetic uniform field B_O. To the average magnetic field B_O, a perturbation is added. In particular, starting from the characteristic of superdiffusive transport described by Lévy Walk model discussed in the previous chapters

(i.e. Chapter 3 and Chapter 4), the motion is analyzed by a diffusion law

$$\langle \Delta x_i^2(t) \rangle = 2D_\alpha t^\alpha \tag{5.35}$$

where Δx_i represents the deviation of the $i-th$ coordinate from the initial position at time t, and the coefficient D_α, has the dimensions of a speed for a length. In the case of normal diffusion (i.e Gaussian-type) $\alpha = 1$. So that, to evaluate the transport of the particles we have built a Monte-Carlo simulation, which integrates the equations along the Parker spiral adding to each integration step a disturbance (i.e. random noise) corresponding to the model of Lévy Walk, in order to take into account the effect of the inhomogeneity of the magnetic field in the solar wind. The equations to be integrated can be represented by the following Langevin equation

$$\frac{d\vec{r}}{dt} = \vec{v}_0 + \delta\vec{v} \tag{5.36}$$

where $\vec{v}_0$ is the average velocity field and $\vec{v}$ is the fluctuation of this field due to turbulence. The disruption is evaluated locally, taking into account the expression obtained for the diffusion coefficient in Lévy Walk model discussed in Chapter 4.

5.3   Numerical code details

The Figure 5.1 shows the structure of the code The main module, which uses the input parameters, synchronize the different stages of the process invoking the functions for the motion simulation, organized in a consistent manner with the context. The process of implementation can be summarized thus:

- reading of the input parameters (the physical parameters of the particles, the quantity of particles, duration of the simulation, parameters for the statistics of Lévy)

- Injection of particles

- Integration of the equations of the motion of particles

- Perturbation of the trajectories by using the model of Lévy Walk

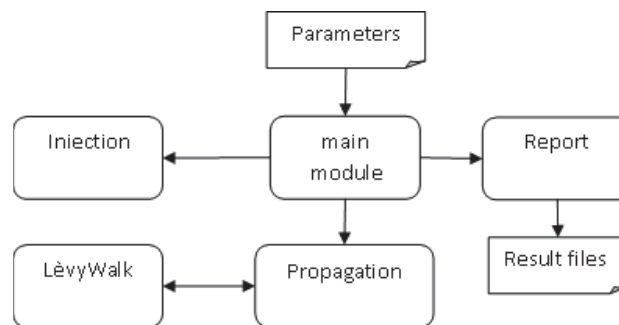- Generation of output data (trajectories and statistics)

Figure 5.1 Numerical code structure

Two main groups of codes were then generated, one for the integration of the equations of motion in spherical coordinates (ie Propagation), the other for the generation of the perturbation using the model of Lévy Walk (i.e. Lévy Walk).

The routines for the simulation of the motion in approximation of drift belong to the first group of programs. The code is based on a Runge-Kutta integration routine used by a subroutine that implements the equations of motion to be integrated in spherical coordinates (ref. dimensionless equations of motion in spherical coordinates).

The second group of programs implements the model of Lévy Walk for the generation of random numbers for which the statistical distribution is of Maxwellian type with decay of the polynominal lines(ref. to the Lévy statistics). The parameters used for the simulation are:

- number of particles to be used in the simulation

- number of cycles of temporal integration (i.e. duration of the motion of particles)

- charge of the particle

- mass of the particles

- distance for positioning the detector

- sampling rate for the production of the histograms

- size of the bin for the production of the histograms

- μ, exponent of the diffusion equation

5.4   Numerical results

The verification of the code has been carried out through the launch of different run increasing the number of particles and the time cycles, as well as injecting particles at different energies. For each run, in addition to the visualization of the trajectories, was made a measurement of the particle stream at a distance of 1 AU to verify statistical distributions. There have been several run carried out by varying the input parameters of the number of particles to their energy characteristics and ending with the characterization of the exponent in the diffusion equation. Regarding the trajectories (fig. trajectories), simulations have been carried out by injecting tens of particles with different energies (ie different values of charge and mass) and, for the same energy, with different values of diffusion equation exponent (i.e. μ).
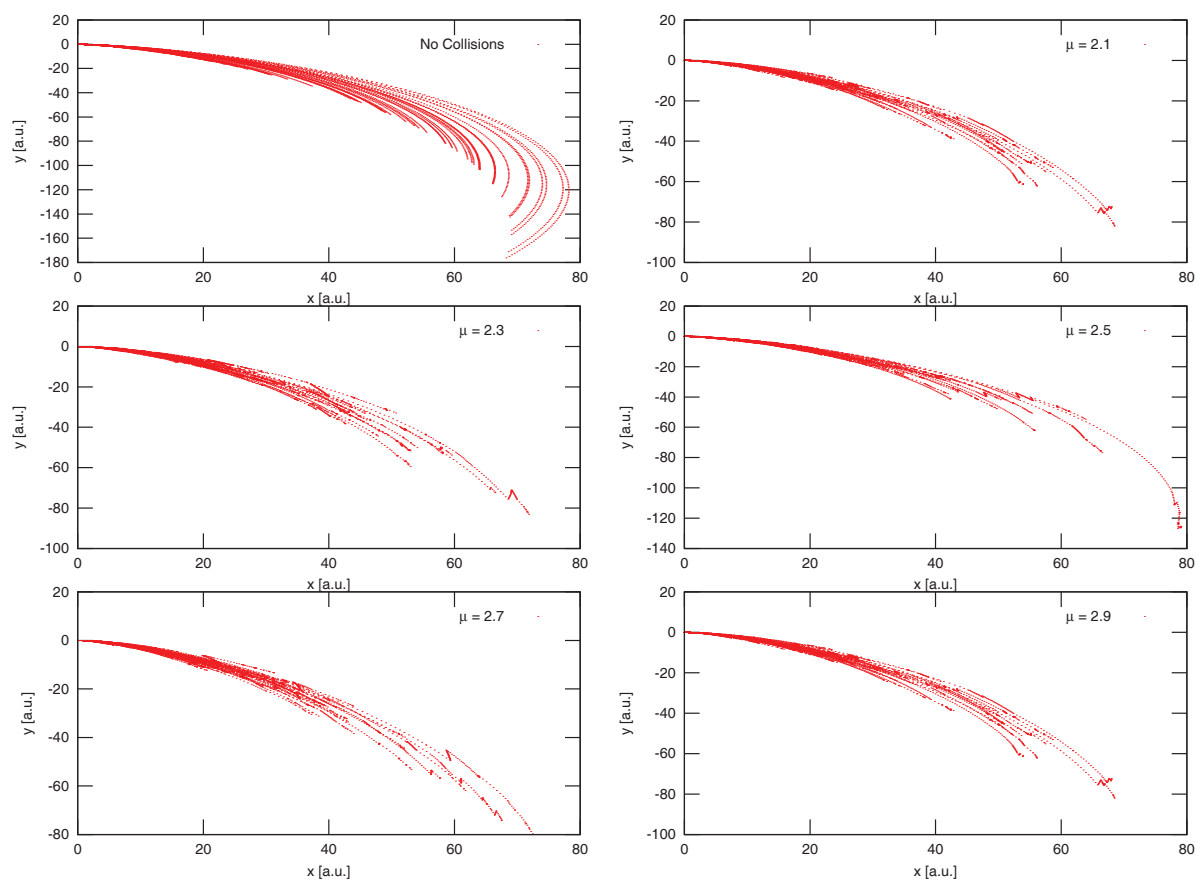
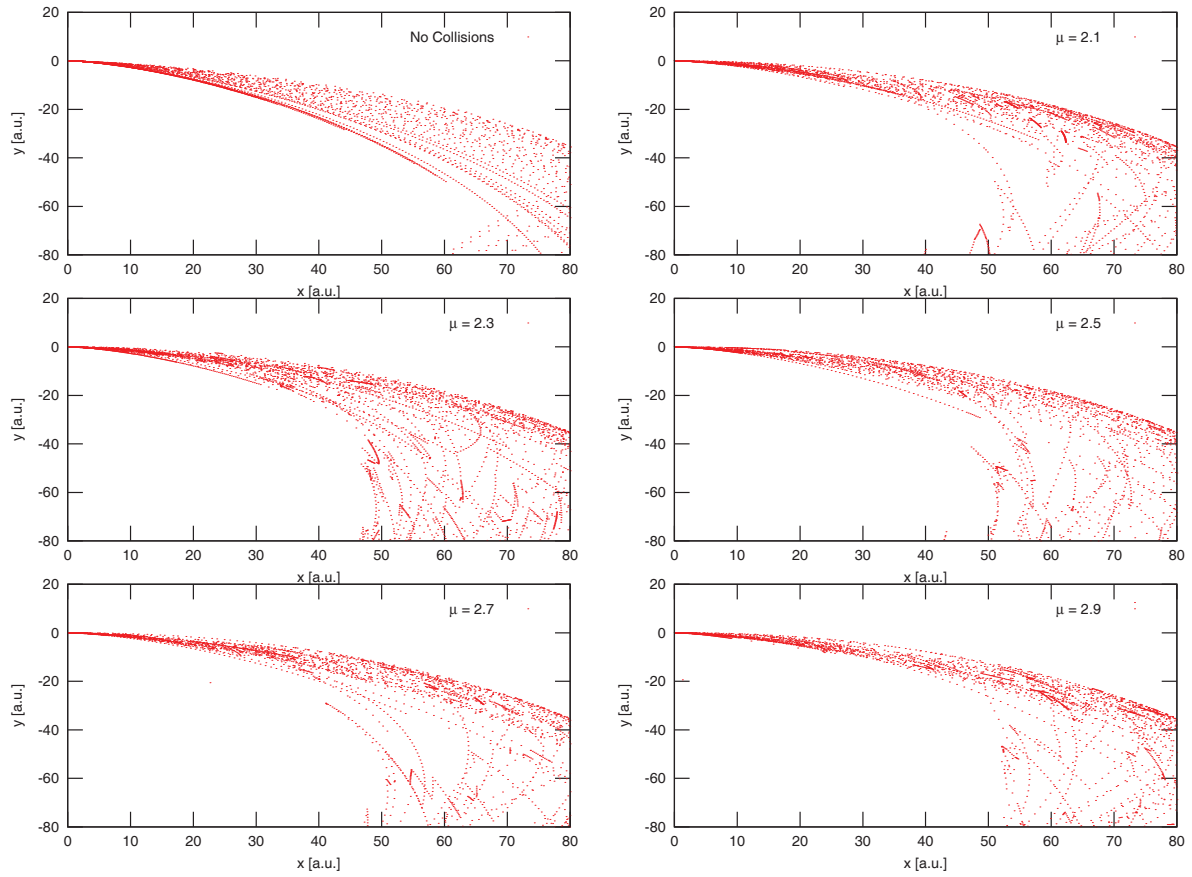**Figure 5.2** Trajectories with different values of μ for particles with $E = 0.01 MeV$

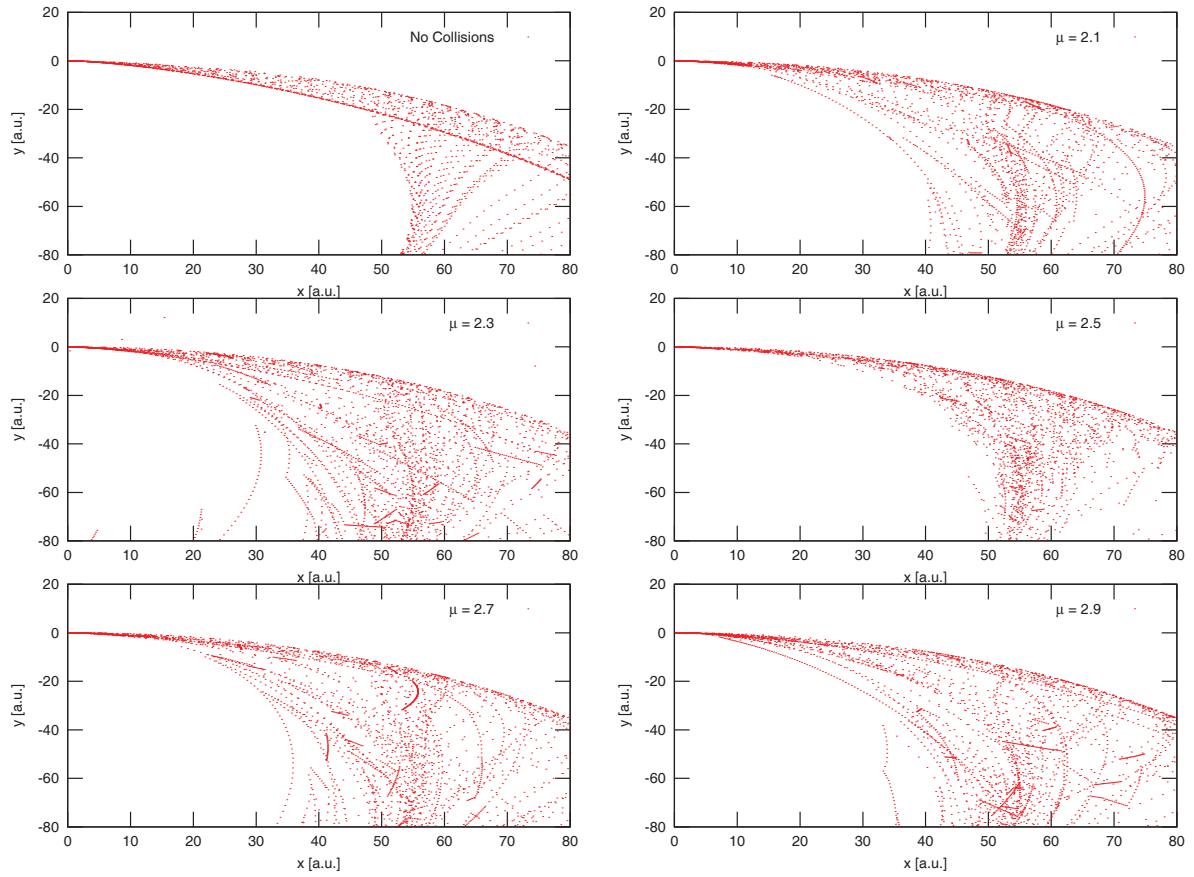**Figure 5.3** Trajectories with different values of μ for particles with $E = 0.15 MeV$

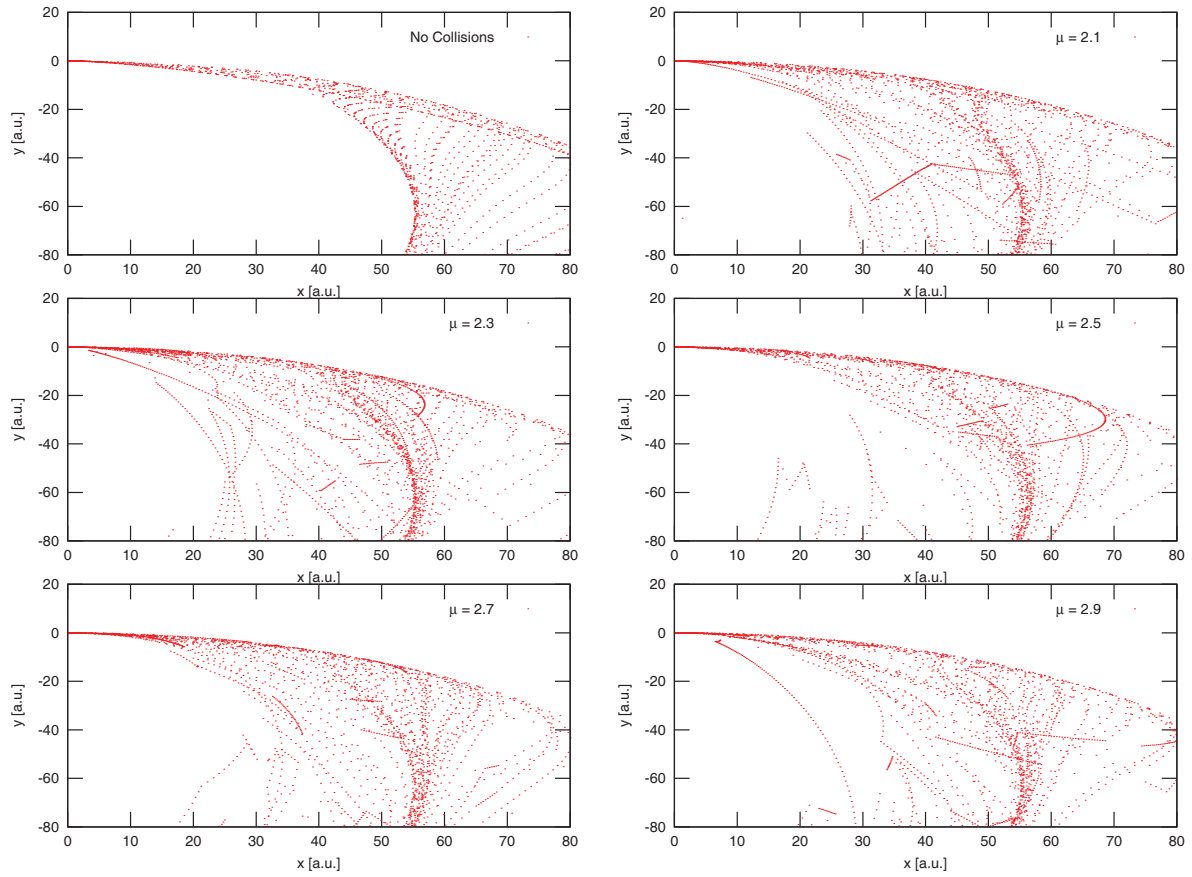**Figure 5.4** Trajectories with different values of μ for particles with $E = 0.5 MeV$

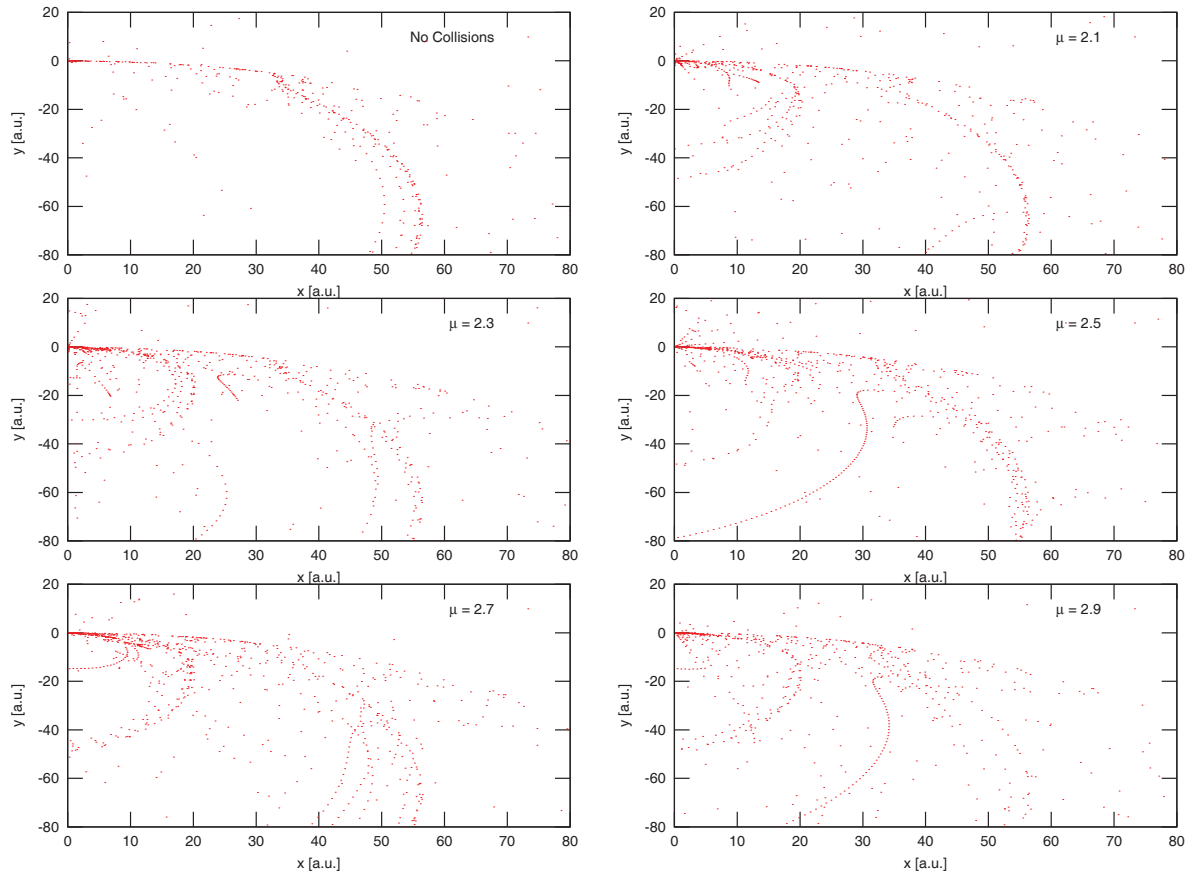**Figure 5.5** Trajectories with different values of μ for particles with $E = 1MeV$

Figure 5.6 Trajectories with different values of μ for particles with $E = 16MeV$
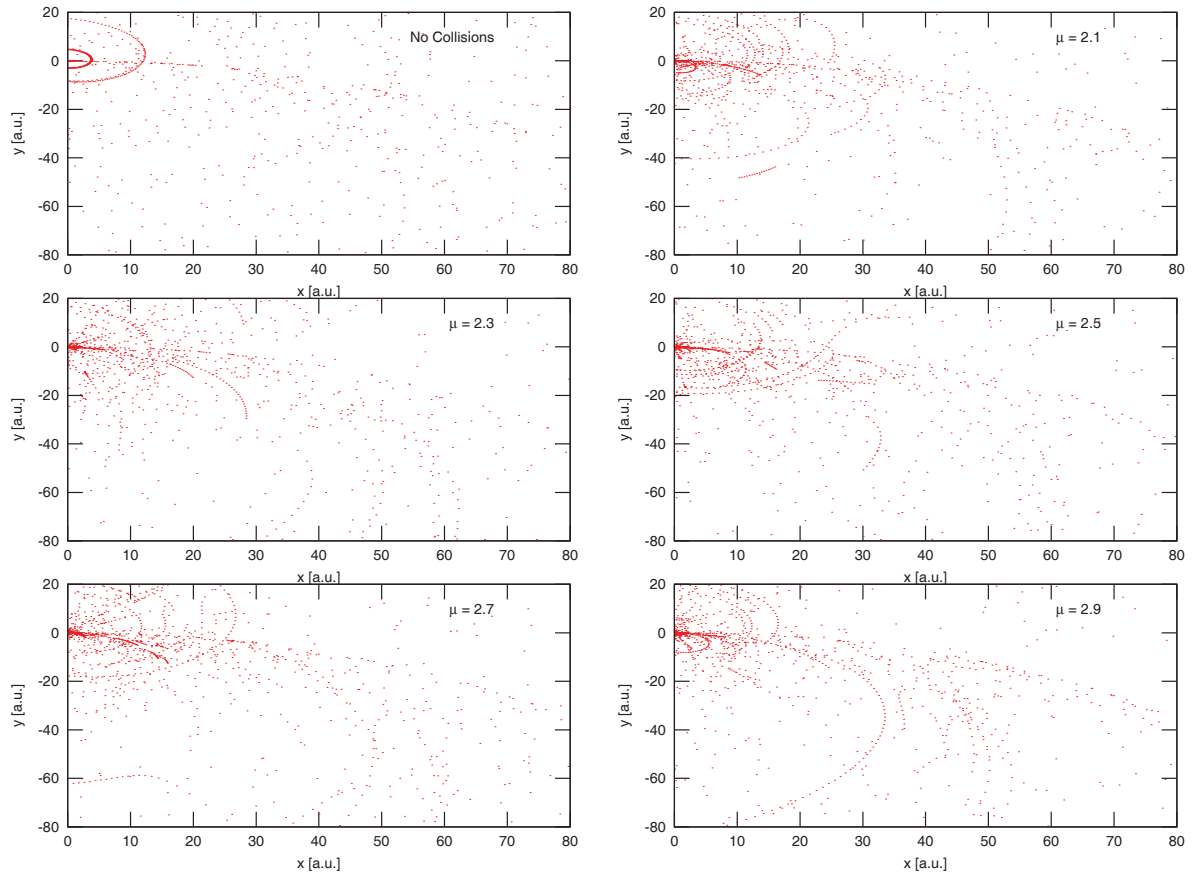
Figure 5.7 Trajectories with different values of μ for particles with $E = 33MeV$

As shown in the figures (Fig. 5.7) , we note that varying the exponent for the generation of the perturbations according to the model of Lévy for the same energy , the perturbation modifies the trajectories of the particles carrying them further away as the characteristics of the superdiffusive motion are approached (i.e. *mu* > 2) and further away from the normal distribution (i.e. *mu* = 2). The particularities of the transport were studied by injecting a large number of particles (about 1 million) and " placing " a detector at a distance of 1 AU or constructing the distribution at the distance of an 1 AU as if it was present a detector of energetic particles (an example is given in Fig. 5.8) . As it has been done for trajectories , also for the study of transport we are performing various simulations varying the energy of the particles and , for the same energy , the exponent of the diffusion equation. The goal for this series of simulations is to obtain an accurate data set for
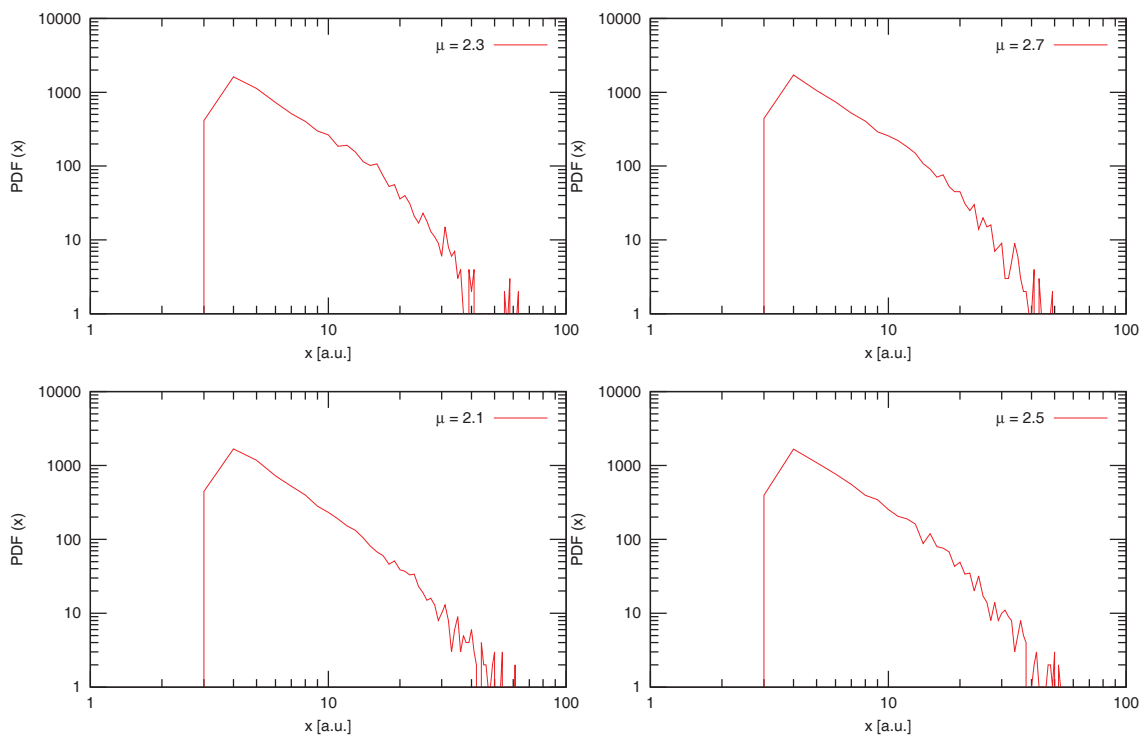

Figure 5.8 Particle fluxes with different values of μ

comparison between the observed data by satellite and the numerical results. In particular, one can

note the following features: the variation of μ varies the slope of the histogram, the histograms show the typical form of the power-law tails distributions. The forthcoming simulations will allow to build up a database of computed time profiles to compare with the spacecraft observations. This will allow to determine the energetic particle transport properties in the various cases.

5.5   Numerical results *vs* observed data

The comparison between the observed data from the satellites and the numerical simulations designed, is, as mentioned earlier, the final goal of our work. The characteristics of the transport of energetic particles appear to be central to the issues related to space weather, with particular reference to the possibility of predicting damaging phenomena to the equipment that orbit around our planet. From the methodological point of view, we started the study of the motion of these particles in spherical coordinates to get to determine the characteristics of the transport models using Lévy Walk, that have described the characteristics of transport for particle fluxes observed by satellites. At the moment we have not yet fully achieved the goal in the sense that we have not had the opportunity to apply our models to both the dynamics of impulsive events and the dynamics of gradual events. In any case, we were able to produce the first comparisons by examining the pulse previously analysed (ref. chapter 2) and constructing simulations that reproduce the physical characteristics of the particles involved (FIG. comparison simulation-data)
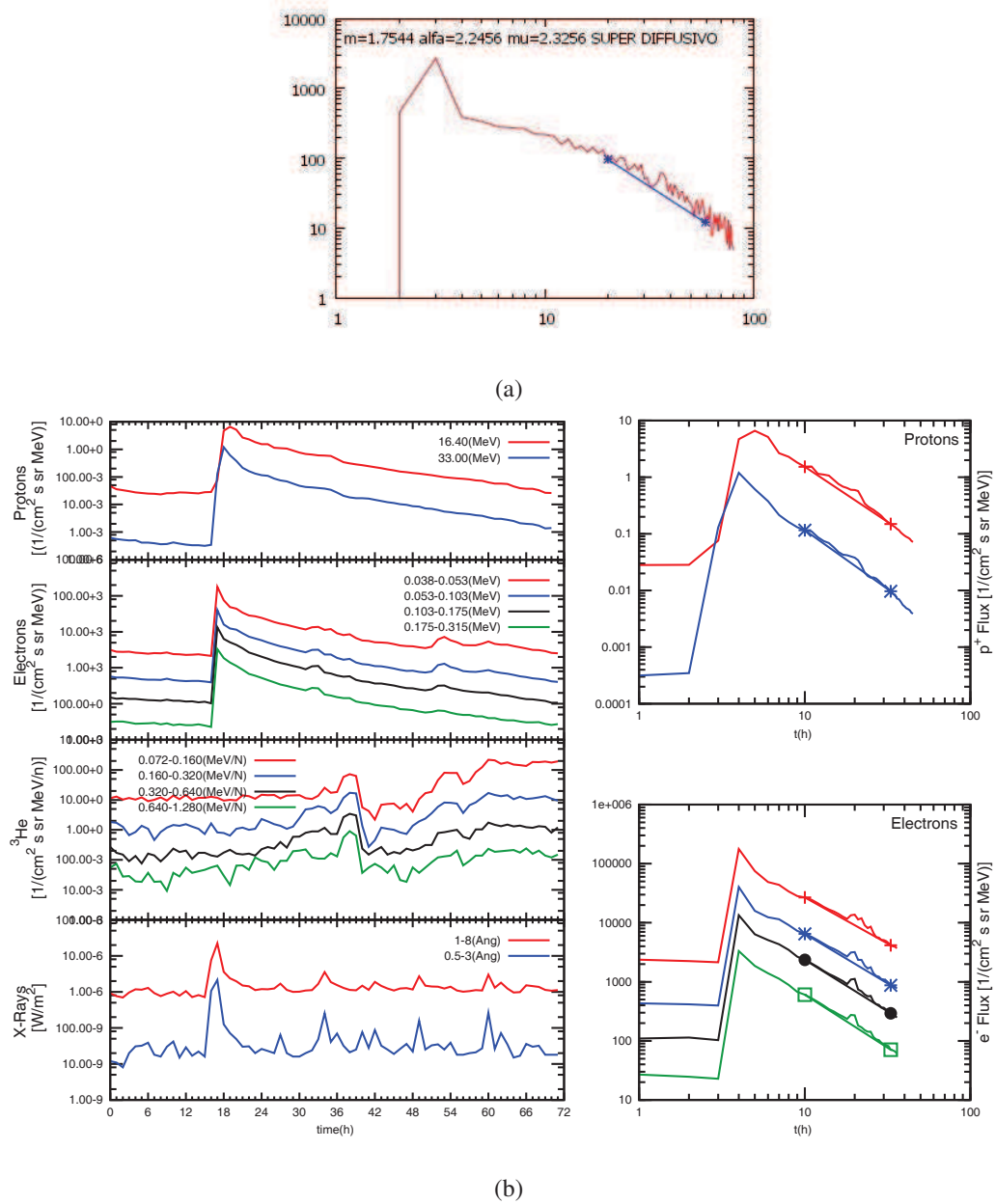
(a)

(b)

Figure 5.9 Satellite Data vs numerical results.: (a) numerical simulation; (b) impulsive event;

Chapter 6

Conclusions

In this work we have developed a methodology and a numerical model to extract information about the transport of solar energetic particles. Starting from the analysis of satellites data (i.e. energetic particle fluxes), we have build a numerical model that integrates both the peculiar characteristics of the motion of these energetic particles in the solar wind, either the characteristics of the transport especially for the emission of energetic particles linked to the presence of impulsive events onm the Sun (i.e. flares).

In the first part of the work we have developed a method to extract information on the transport of solar energetic particles by analysing the time decay of the energetic particles fluxes measured by spacecraft in the solar wind. Our aim was to highlight the existence of superdiffusive transport regime, intermediate between normal diffusion and ballistic transport. To this end, we considered the different forms of the propagator for the different transport regime. It has been shown that for superdiffusive transport along the magnetic field, in the limit of long times, the particle flux decays as a power law with exponent m, where m is related to μ by $\mu = m/(m-1)$, and the anomalous diffusion exponent is given by $\alpha = 4 - \mu$. Therefore, $3/2 < m < 2$ corresponds to superdiffusion. We analysed the time profiles of a number of impulsive SEPs and found superdiffusive and ballistic transport regimes, both for electrons and protons. In the above analysis, we assumed that the

energetic electrons and ions are injected as a δ-function in space and time. From the X ray peaks in Fig. 2.4, 2.5, and 2.6, we can estimate the injection time at the source to be about 2–3 h, which is much less than the duration of the SEP event at the observer, about 50 hours. For this reason we assume that the particle emission at the source can be represented by a delta function, from which it follows that the propagator corresponds to the observed particle profile. It is interesting to notice that, if the particle injection is not a delta function, but there is a tail in the emission profile $f(t)$, this will contribute to the observed flux at late times. In this case, this means that the observed decay of the particle flux is not as steep as it would be for a delta function injection, because of the contribution of "late" particles. A steeper decay implies a higher value of m (see Eq. (15)), hence higher values of α, so we can say that the reported values of α for the superdiffusive cases are lower estimates. For protons, we find ballistic, i.e., scatter-free, transport in one case and normal diffusion in another case. It should be noted that different proton energies were considered in those two cases, i.e., 16-33 MeV in the event of June 10, 2000, and 0.1-1.0 MeV for the event of February 20, 2002. Such different transport regimes can depend both on the particle gyroradius (e.g. Pommois et al. (2007)) and on the turbulence level, and are consistent with the variety of proton mean free paths considered, for instance, by Chollet et al. (2010). For the electrons in the energy channels from 0.01 to 0.32 MeV, we find superdiffusive transport with the exponent α ranging from 1.22 to 1.73, and ballistic or quasi-ballistic transport as well. These regimes complement those found by Perri and Zimbardo (2008a;b; 2009a), where anomalous diffusion exponent α from 1.1 to 1.6 were obtained, and show that a wide range of anomalous diffusion exponents $1 < \alpha < 2$ is possible and that superdiffusive transport can be the most frequent regime for energetic electrons. Furthermore, we also find that scatter-free transport can be interpreted in terms of the propagator and the jump probability for Levy random walk with $\mu < 2$, a regime that we call quasi-ballistic. We should mention that in the above analysis we have neglected the effects of adiabatic deceleration, which leads to a decrease in time of particles with a given energy. This effect

should be negligible for SEPs, as suggested by Gombosi (1979). Indeed Ruffolo (1995) finds a typical time for adiabatic deceleration of six days at 1 AU, which is much longer than the typical decay times of the analysed events. More recently Chollet et al. (2010) found by a numerical simulation that the average energy loss for a 1 MeV proton reaching 1 AU, assuming a mean free path $\lambda = 0.10 - 0.30 AU$, is 30%, which is a bit less than with the energy width of the energy channels considered above. This shows that adiabatic deceleration can be neglected in a first analysis.

The finding that both electrons and protons can exhibit a variety of transport regimes that are different from normal diffusion can be related to the fact that the magnetic turbulence level in the solar wind, which determines the amount of pitch angle scattering, actually varies considerably from event to event (see for instance the values of $\delta \vec{B}/B_0$ reported by (Ippolito et al. 2005) for several solar flares and associated SEPs events). Likewise, recent data analysis shows that magnetic turbulence in the slow solar wind, where both SoHO and ACE spend most of time, is frequently only weakly stationary (Perri and Balogh 2010a). A comparison of the obtained transport regime with the observed turbulence properties would be interesting, but a spacecraft can measure the fluctuation transported by the solar wind in the radial direction, while the particles propagate along the Parker spiral, so that a direct comparison is not easy. The obtained results imply that, beside diffusive transport and scatter-free transport, superdiffusive transport is also possible for electrons accelerated at impulsive SEPs event. This finding is obtained from the analysis of experimental data, and it confirms the predictions of superdiffusive or nearly ballistic transport of numerical simulations as reported by (Pommois et al. 2007; Shalchi and Kourakis 2007; Zimbardo et al. 2006). Therefore a substantial rethinking of SEPs propagation is necessary, because it can influence both the acceleration mechanism and the predictions of electrons and protons fluxes required by space weather reports and the assessment of the amount of total energy required to accelerate particles at impulsive events, as determined from the observed particle fluxes.

After the data analysis, we have developed a numerical model of the Lévy random walk. The

model depends on three clearly identified parameters, the power-law exponent μ of the tails of the free path probability distribution Ψ, the distance x_0 beyond which Ψ is a power law, and the particle speed v. The above numerical study has shown that a random walk described by a Lévy law including the space-time coupling is able to reproduce the theoretical prediction for Lévy walks, and in particular superdiffusion with the anomalous diffusion exponent $\alpha = 4 - \mu$ for $2 < \mu < 3$, as well as the propagators $P(x,t)$ with power law tails. We illustrate now two potential applications of the above derived algorithm. The first regards the propagation in the interplanetary space of particles accelerated at a coronal mass ejection driven shock wave. Such a shock wave is considered to be at the origin of gradual SEP events: since the shock wave is traveling outward from the sun and is evolving (usually becoming weaker), the flux of energetic particles detected by a spacecraft is the superposition of those emitted at the shock in different places and times. However, both the source strength and the propagation properties can vary during the shock evolution. Therefore, an application of the analytical propagators to data analysis is not immediate, and a numerical algorithm is necessary. Conversely, in the case of impulsive SEPs, the source of energetic particles can be approximated by a delta function and the density time profile is approximately given by the propagator, as shown by Trotta and Zimbardo (2011). For gradual SEP events, proper modeling of the time evolution of the shock source and of the propagation properties in the inhomogeneous solar wind can allow to compute the energetic particle profile, which can then be compared to the observations. Clearly, for modeling superdiffusive propagation in a medium where the properties are changing, a flexible Lévy walk model, where μ and x_0 are readily accessible, is needed. A recent study indicates how the free path probability parameters can be obtained from the analysis of magnetic fluctuations in the solar wind (Perri and Zimbardo 2012a). The second application concerns the acceleration of cosmic rays according to the model of superdiffusive shock acceleration (SSA) (Perri and Zimbardo 2012b), which predicts an energy spectral index γ which depends both on the shock compression ratio $r = V_1/V_2$, with V_1 and V_2 the upstream and the downstream

plasma speeds, respectively, and on the exponent of superdiffusion α; for ultrarelativistic particles this is found to be (Perri and Zimbardo 2012b; Perrone et al. 2013)

$$\gamma = \frac{6}{r-1}\frac{2-\alpha}{3-\alpha} + 1 \tag{6.1}$$

This spectral index recovers that of diffusive shock acceleration (DSA) in the limit of normal diffusion, $\alpha = 1$. While the theoretical derivation of SSA has been given by Perri and Zimbardo (2012b), it would be interesting to reproduce the spectral index γ by a numerical simulation of Lévy random walk, as implemented here, in the presence of a shock wave and of the corresponding velocity jump from V_1 to V_2. The numerical simulation would allow to investigate the effects on varying boundary condition upstream and downstream of the shock (e.g., Ostrowski and Schlickeiser 1996). In conclusions, we have developed a numerical algorithm which allows to generate a Lévy random walk, as opposed to a simpler Lévy flight process. The algorithm is able to reproduce the expected mean square displacement, growing superdiffusively, and the expected propagator, having power-law tails. The parameters which govern the random walk and the superdiffusive behaviour, that is μ, x_0, and v, are clearly identified and have an immediate physical meaning. This makes the algorithm easy to use and appropriate for further modeling of more complicated, in particular nonhomogeneous, systems.

The final part of the work was devoted to the construction of case studies to the "validation" of the model, starting from the comparison with energetic particles emitted by impulsive events whose results were shown in the previous chapter. The development in a more immediate future could be the study of gradual events, ie events for which the source of particles cannot be considered punctual.

Ultimately this work can be considered the starting point for the analysis of different transport regimes related to the propagation of energetic particles in the solar wind for both impulsive events that gradual events. Of particular relevance and originality is the study of transport based on Levy-Walk models that assume this coupling space-time in the evolution of the particle motion that

seems to well describe the characteristics of super-diffusive transport.

Bibliography

Bitane, R., Zimbardo, G., Veltri, P., , Astrophys. J. 719 (2010) 1912.

Blumen, A., Klafter, J., Zumofen, G., A stochastic approach to enhanced diffusion: Lévy walk., Europhys. Lett. 13 (1990) 223-229.

Bouchaud, J. P., Georges, A., Anomalous diffusion in disordered media: Statistical mechanisms, models and physical applications., Phys. Rep. 195 (1990) 127-293.

Chollet, E.E., Giacalone, J., Mewaldt, R.A., , J. Geophys. Res. 115 (2010) A06101.

Consolini, G., Kretzschmar, M., Lui, A. T. Y., et al., On the magnetic field fluctuations during magnetospheric tail current disruption: A statistical approach., J. Geophys. Res. 110 (2005) A07202 doi: 10.1029/2004JA010947.

Dalla, S., Balogh, A., Krucker, S., , Annales Geophys. 21 (2003) 1367.

Dalla, S., Agueda, N., Twelfth International Solar Wind Conference, AIP Conf. Proc. 1216 1216 (2010) 613-616.

del-Castillo-Negrete, D., Carreras, B. A., Lynch, V. E., Fractional diffusion in plasma turbulence, Phys. Plasmas 11 (2004) 3854-3864.

Duffy, P., Kirk, J. G., Gallanta, Y. A., Dendy, R.O., , Astron. Astrophys. 302 (1995) L21-L24.

Effenberger, F., Anisotropic Diffusion of Energetic Particles in Galactic and Heliospheric Magnetic Fields., PhD Thesis, Bochun, 2012.

Friedrich, T., Jenko, J., Baule, A., Eule, S., , Phys. Rev. Lett. 96 (2006) 230601.

Galloway, R.K., Helander, P., MacKinnon, A.L, Dendy, R.O., , Astrophys. J. 646 (2006) 615.

Geisel, T.; Nierwetberg, J.; Zacherl, A. Accelerated diffusion in Josephson junctions and related chaotic systems, Phys. Rev. Lett. 54 7 (1985) 616-619.

Ghaemi, M., Zabihinpour, Z., Asgari, Y., Computer simulation study of the Levy flight process, Physica A 388 (2009) 1509-1514.

Giacalone, J., Jokipii, J.R., , Astrophys. J. 520 (1999) 204.

Gombosi, T.I.,Physics of the Space Environment, Cambridge University Press (1979) .

Greco, A., Taktakishvili, A. L., Zimbardo, G., Veltri, P., Zelenyi, L. M., Ion dynamics in the near-Earth magnetotail: Magnetic turbulence versus normal component of the average magnetic field, J. Geophys. Res. 107 (2002) SMP 1-1.

Ippolito, A., Pommois, P., Zimbardo,G., Veltri, P., , Astron. Astrophys. 438 (2005) 715.

Klafter, J., Blumen, A., Shlesinger, M. F., Stochastic pathway to anomalous diffusion., Phys. Rev. A 35 (1987) 3081-3085.

Klafter, J., Blumen, A., Shlesinger, M. F., Zumofen, G., Reply to Comment on Stochastic pathway to anomalous diffusion., Phys. Rev. A 41 (1990) 1158-1159.

Krucker, S., Lin, R.P., , Astrophys. J. 542 (2000) L61.

Krucker, S., Oakley, P.H., Lin, R.P., , Astrophys. J. 691 (2009) 806.

Lee, M.A, Fisk, L.A., Shock acceleration of energetic particles in the heliosphere., Solar Physics 32 (1982) 205-228.

Lin, R.P., , Space Sci. Rev. 16 (1974) 189.

Lin, R.P., , Adv. Space Res. 35 (2005) 1857.

McKibben, R.P., , Adv. Space Res. 35 (2005) 518.

Metzler, R., Klafter, J., The random walk's guide to anomalous diffusion: a fractional dynamics approach., Phys. Reports 339 (2000) 1-77.

Metzler, R., Klafter, J., Topical review: The restaurant at the end of the random walk: recent developments in the description of anomalous transport by fractional dynamics., J. Phys. A: Math. Gen. 37 (2004) R161-R208.

Müller-Mellin, R., Kunow, H., et al., , Solar Phys. 162 (1995) 483.

Nisticó, G., Bothmerv, V., Patsourakos, S., Zimbardo, G., , Solar Phys. 259 (2009) 87.

Ostrowski, M., Schlickeiser, R., Cosmic-ray diffusive acceleration at shock waves with finite upstream and downstream escape boundaries., Solar Phys. 169 (1996) 381.

Perri, S., Balogh, A., Stationarity in solar wind flows.m Astrophys. J. 714 (2010) 937-943.

Perri, S., Balogh, A., Characterization of transition in solar wind parameters., Astrophys. J. 710 (2010) 1286-1294.

Perri, S., Zimbardo, G., Evidence of superdiffusive transport of electrons accelerated at interplanetary shocks., Astrophys. J. Lett. 671 (2007) 177-180.

Perri, S., Zimbardo, G., Superdiffusive transport of electrons accelerated at corotating interaction regions., J. Geophys. Res. 113 (2008) A03107 doi:10.1029/2007JA012695.

Perri, S., Zimbardo, G., , Astrophys. Space Sci. Trans. (ASTRA) 4 (2008) 27.

Perri, S., Zimbardo, G., Ion and electron superdiffusive transport in the interplanetary space., Adv. Space Res. 44 (2009a) 465-470.

Perri, S., Zimbardo, G., Ion Superdiffusion at the Solar Wind Termination Shock, Astrophys. J. Lett. 693 (2009b) L118-L121.

Perri, S., and Zimbardo, G., Magnetic Variances and Pitch-angle Scattering Times Upstream of Interplanetary Shocks, Astrophys. J. 754 (2012a) 8.

Perri, S., and Zimbardo, G., Superdiffusive Shock Acceleration, Astrophys. J. 750 (2012b) 87.

Perrone, D., Dandy, R.O., Furno, I., et al., Nonclassical transport and particle-field coupling: from laboratory plasma to the solar wind., Space Sci. Rev. in press (2013)

Pommois, P., Zimbardo, G., Veltri, P., Anomalous, non-Gaussian transport of charged particles in anisotropic magnetic turbulence., Phys. Plasmas 14 (2007) 012311-1–012311-11.

Pommois, P., Zimbardo, G., Veltri, P., , Astrophys. J. 639 (2007) L91.

Qin, G., Matthaeus, W.H., Bieber, J.W., , Geophys. Res. Lett. 29 (2002a) 1048.

Qin, G., Matthaeus, W.H., Bieber, J.W., , Astrophys. J. 578 (2002b) L117.

Ragot, B.R., Kirk, J.G., , Astron. Astrophys. 327 (1997) 432.

Reames, D.V., , Space Sci. Rev. 90 (1999) 413.

Ruffolo, D., , Astrophys. J. 442 (1995) 861.

Sandroos, A., Vainio, R.O., , Astron. Astrophys. 507 (2009) L21.

Shalchi, A., Kourakis, I., A new theory for perpendicular transport of cosmic rays., Astron. Astrophys. 470 (2007) 405-409.

Shalchi, A., Kourakis, I., , Physics of Plasmas 14 (2007) 112901.

Shlesinger, M. F., West, B. J., and Klafter, J., Levy dynamics of enhanced diffusion: Application to turbulence., Phys. Rev. Lett. 58 (1987) 1100.

Shlesinger, M. F., West, B. J., and Klafter, J., From Bernoulli scaling to turbulent diffusion., Physica Scripta 40 (1989) 445-448.

Shlesinger, M. F., Zaslavsky, G. M., and Klafter, J., Strange kinetics, Nature 363 (1993) 6424.

Sugiyama, T., and Shiota, D., Sign for super-diffusive transport of energetic ions associated with a coronal-mass-ejection-driven interplanetary shock., Astrophys. J. 731 2011 L34-L37.

Tautz, R.C., Simulation results on the influence of magneto-hydrodynamic waves on cosmic ray particles., Plasma Phys. Control. Fusion 52 (2010) 045016.

Teufel, A., Schlickeiser, I., , Astron. Astrophys. 393 (2002) 703.

Trotta, E.M., Zimbardo, G., Quasi-ballistic and superdiffusive transport for impulsive solar particle events., Astron. Astrophys. 530 (2011) A130.

Trotta, E.M., Zimbardo, G., Superdiffusive and ballistic propagation of protons in solar energetic particle events, Proceedings of IAU Symposium 274 (2011) 198-200.

Trotta, E.M., Zimbardo, G., Non diffusive propagation of SEP: data analysis and numerical simulations, Proceedings of ECLA - European Conference on Laboratory Astrophysics 58 (2012) 99-102.

Vlahos, L., Isliker , H., et al., Normal and Anomalous Diffusion: A Tutorial., Preprint submitted to Elsevier (1988) .

Webb, G.M., Zank, G.P., Kaghashvili, E.Kh., Roux, J.A., , Astrophys. J. 651 (2006) 211.

Weeks, E. R., Swinney, H.L., Anomalous diffusion resulting from strongly asymmetric random walks., Phys. Rev. E 57 (1998) 4915-4920.

Zaslavsky, G. M., Chaos, fractional kinetics, and anomalous transport., Phys. Reports 371 (2002) 461-580.

Zhang, M., McKibben, R.B., Lopate, C., et al. , , J. Geophys. Res. 108 (2003) 1154.

Zimbardo, G., Veltri, P., Pommois, P., Anomalous, quasilinear, and percolative regimes for magnetic-field-line transport in axially symmetric turbulence., Phys. Rev. E 61 (2000a) 1940-1948.

Zimbardo, G., Greco, A., Veltri, P., Superballistic transport in tearing driven magnetic turbulence., Phys. Plasmas 7 (2000b) 1071-1074.

Zimbardo, G., Pommois, P., Veltri, P., , J. Geophys. Res. 109 (2004) A02113.

Zimbardo, G., Anomalous particle diffusion and Lévy random walk of magnetic field lines in three-dimensional solar wind turbulence., Plasma Phys. Control. Fusion 47 (2005) B755-B767.

Zimbardo, G., Pommois, P., Veltri, P., Superdiffusive and subdiffusive transport of energetic particles in solar wind anisotropic magnetic turbulence., Astrophys. J. Lett. 639 (2006) L91-L94.

Zimbardo, G., Bitane, R., Pommois, P., Veltri, P., , Plasma Phys. Control. Fusion 51 (2009) 015005.

Zimbardo, G., Greco, A., Sorriso-Valvo, L., et al., Magnetic turbulence in the geospace environment., Space Sci. Rev. 156 (2010) 89.

Zimbardo, G., Perri, S., Pommois, P., et al., Anomalous particle transport in the heliosphere., Adv. Space Res. 49 (2012) 1633.

Zumofen,G., Klafter, J., Scale-invariant motion in intermittent chaotic systems., Phys. Rev. E 47 (1993) 851-863.

ACKNOWLEDGMENTS

Questo e' l'atto finale!

Spinto da Gaia (che e' qui vicino a me), provo a citare le persone che hanno avuto un ruolo in questo percorso.

E' evidente che tutto cio' e' il risultato della caparbieta' ed allora il primo da citare e' Papa', sempre positivo, sempre con lo sguardo in avanti. Mi basterebbe avere nel DNA un briciolo della sua indole.

La caparbieta' da sola non basta; allora diventano fondamentali le persone piu' vicine che ti danno motivazione, supporto e tutto quanto e' necessario per superare i momenti piu' *complessi*: Mariella, Domenico, Gaia e Marta semplicemente fantastici.

Importante, ancora, la dose di orgoglio che ho percepito sempre negli sguardi e nei pensieri di mia madre: meriterebbe molto di piu', ma al momento questo ho potuto fare.

Non ho avuto sorelle (solo (!) 4 fratelli cui voglio tanto bene!), ma come non pensare a lei come se lo fosse ?! Grazie Mari (Maria Giovanna) per tutto il supporto linguistico (e non solo ...).

Va da se che la parte scientifica senza il Prof. Zimbardo non si sarebbe mai fatta: grazie 1000.

Nella vita non *vivo di Fisica* (e questo forse mi dispiace!), ma avere avuto la possibilita' di avvicinarmi a questo mondo e' stato senza dubbio entusiasmante. Oltre alla *bellezza* delle cose che ho studiato, resta la bella sensazione legata alla possibilita' di raggiungere un obiettivo in maniera indipendente da ogni tipo di condizionamento (eta', lavoro, ecc.). E' bello conoscere, ed ancora piu' bello se lo si puo' fare senza una finalita' diversa dal conoscere stesso.